1948 *20 Years of Research Progress* 1968

ARL 68-0067
APRIL 1968

Aerospace Research Laboratories

ELECTRIC ARCS IN TURBULENT FLOWS, III

GERHARD FRIND
BEN LEE DAMSKY
GENERAL ELECTRIC COMPANY
PHILADELPHIA, PENNSYLVANIA

Contract No. F33-615-67-C-1374
Project No. 7063

OFFICE OF AEROSPACE RESEARCH
United States Air Force

63

NOTICES

When Government drawings, specifications, or other data are used for any purpose other than in connection with a definitely related Government procurement operation, the United States Government thereby incurs no responsibility nor any obligation whatsoever; and the fact that the Government may have formulated, furnished, or in any way supplied the said drawings, specifications, or other data is not to be regarded by implication or otherwise as in any manner licensing the holder or any other person or corporation, or conveying any rights or permission to manufacture, use, or sell any patented invention that may in any way be related thereto.

Agencies of the Department of Defense, qualified contractors and other government agencies may obtain copies from the

Defense Documentation Center
Cameron Station
Alexandria, Virginia 22314

This document has been released to the

CLEARINGHOUSE
U.S. Department of Commerce
Springfield, Virginia 22151

for sale to the public.

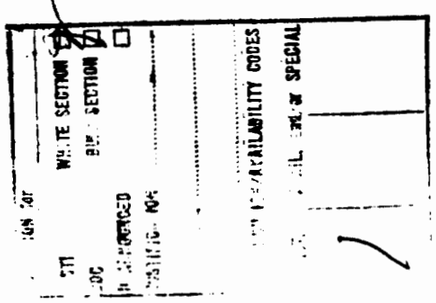

Copies of ARL Technical Documentary Reports should not be returned to Aerospace Research Laboratories unless return is required by security considerations, contractual obligations or notices on a specified document.

400 - August 1968 - CO455 - 45-926

ARL 68-0067

ELECTRIC ARCS IN TURBULENT FLOWS, III

GERHARD FRIND
BEN LEE DAMSKY

GENERAL ELECTRIC COMPANY
PHILADELPHIA, PENNSYLVANIA

APRIL 1968

Contract No. F33-615-67-C-1374
Project 7063

AEROSPACE RESEARCH LABORATORIES
OFFICE OF AEROSPACE RESEARCH
UNITED STATES AIR FORCE
WRIGHT-PATTERSON AIR FORCE BASE, OHIO

FOREWORD

This interim report was prepared by the Engineering Research Section of the General Electric Company, Power Transmission Division, Philadelphia, Pennsylvania on Contract F 33 615 67 C 1374 for the Aerospace Research Laboratories, Office of Aerospace Research, United States Air Force. The work reported herein was accomplished on Task 7063-03, "Energy Exchange Phenomena in Electric Arc Discharges" of Project 7063, "Mechanics of Flight" under the technical cognizance of Col. D. E. Dye of the Thermo-Mechanics Research Laboratory of ARL.

The work was started in February, 1967 and the report manuscript was completed in March, 1968.

The authors wish to acknowledge the able support of Messrs. L. Theil and V. L. Harvey, who assisted in design changes of the apparatus and in the collection of data.

The authors also thank Messrs E. J. Tuohy and B. P. Burgess for performing the Abel transformation and for other computer work, Dr. C. H. Marston for his calculation and design of the heat flux calorimeter described in the appendix, and Dr. T. H. Lee for his continued support and encouragement.

Critical discussions were also conducted with members of the Thermo-Mechanics Research Laboratory and the authors would like, in particular, to thank Mr. P. W. Schreiber for his help in focussing of problems.

ABSTRACT

Work is reported on the development of methods to measure arc temperature, axial pressure gradient, plasma flow velocity and radiative heat flux in long cylindrical turbulent arcs.

Axis temperature and radial temperature distribution of laminar and turbulent 50 amp. nitrogen arcs of 11.2 atm. pressure were found to be of similar size, with some reservation about the accuracy of the "side on" turbulent temperature measurement. The problem of measuring average turbulent arc temperatures was discussed; measurements in "end on" observation and the use of the Milne-Larentz method appear to give better results than "side on" observation of absolute line intensities.

Measurements of the pressure gradient in a 11.2 atm., 125 amp. argon arc show a 1.8 power dependence of pressure gradient on flow rate, indicating that this relationship, well known from cold flow experiments, also holds under the conditions of our experimental arc temperatures.

Plasma velocities were measured by time sequential photography of the turbulent arc structure.

TABLE OF CONTENTS

Section			Page
1.	INTRODUCTION		1
	1.1	General Remarks	1
	1.2	Estimate of Reynolds Numbers in High Flow Speed Nitrogen Arcs	1
2.	IMPORTANCE OF FULLY DEVELOPED FLOW AND DEFINITION OF GOAL OF INVESTIGATION		4
	2.1	Fully Developed Flow	4
	2.2	Goal of Investigation	6
3.	APPARATUS		8
4.	EXPERIMENTS		8
	4.1	Measurements of Potential Gradients	8
	4.11	Methods	8
	4.12	Results	9
	4.2	Measurements of Pressure Gradients	11
	4.21	Methods	11
	4.22	Results	14
	4.3	Measurements of Plasma Velocity	17
	4.31	Methods	17
	4.32	Results	20
	4.4	Measurements of Arc Temperature	24
	4.41	Methods	24
	4.411	Effect of Intensity Fluctuations on Measurement of Average Temperature	24
	4.412	Spectroscopic Instrumentation	28
	4.413	Specific Problems	33
	4.414	Calculation of Relative N_2 Band Line Intensity	33
	4.42	Results	36
	4.421	Temperature of a 50 Amp. 11.2 Atm. Laminar Nitrogen Arc	36
	4.422	Temperature of a 50 amp. 11.2 atm. Turbulent Nitrogen Arc	38
	4.423	Determination of Copper Contamination	41
5.	CONCLUSIONS		41
	5.1	Plasma Pressure	41
	5.2	Plasma Velocity	41
	5.3	Plasma Temperature	41
	5.31	"End on" Observation	41
	5.32	Side on Observation	42

TABLE OF CONTENTS (Cont'd)

Section			Page
	5.33	Laminar and Turbulent Temperature	42
	5.34	Characteristics	42
	5.36	Total Radiative Heat Flux	42
6.	FUTURE WORK		42
7.	APPENDIX		43
8.	REFERENCES		48

LIST OF ILLUSTRATIONS

Figure		Page
1.	Kinematic Viscosity of Nitrogen Plasma	2
2.	Kinematic Viscosity of Argon Plasma	4
3.	Development of an Arc in Coaxial Flow, Schematic Drawing	5
4.	Cascade Arc Constrictor with Window for Spectral Observation	7
5.	Potential Along Length of Arc Constrictor	9
6.	Characteristics of Argon Arcs at 11.2 Atm.	10
7.	Characteristics of Nitrogen Arcs at 11.2 Atm.	11
8.	Pressure Tap, Schematic Drawing	13
9.	Components of Pressure Tap	14
10.	Pressure Along Cylindrical Argon Arc	15
11.	Dependence of Pressure Gradient on Arc Current	16
12.	Dependence of Pressure Gradient on Flow Rate, Turbulent Regime	17
13.	Quartz Window Used for Photographic Determination of Plasma Velocities	18
14.	Electronic Operation of Image Converter Camera System	19
15.	Image Converter Photographs of Argon Arcs Showing the Influence of Flow Rate	21
16.	Sequential Image Converter Photographs of a Turbulent Argon Arc	22
17.	Plasma Velocity as a Function of Arc Current	23
18.	Plasma Velocity as a Function of Flow Rate	24
19.	Spectral Intensity as a Function of Temperature, Schematic	25

LIST OF ILLUSTRATIONS (Cont'd)

Figure		Page
20.	Spectral Intensity as a Function of Temperature, Schematic	27
21.	Optical Ensemble for Photography of Arc and Intensity Standard, Schematic Drawing	29
22.	Views of Spectral Window	30
23.	Example of a Spectrographic Plate	31
24.	Intensity Distribution Before Abel Inversion	32
25.	Relative Intensity of $\lambda = 3371\text{Å}$ Band Lines as a Function of Temperature	35
26.	Variation of the Maximum of the $\lambda = 3371\text{Å}$ N_2 Band Line Intensity with Pressure	36
27.	Line Intensity versus Radius as Determined by Abel Inversion of I(x)	37
28.	Radial Temperature Distribution of a 50 Ampere Nitrogen Arc	39
29.	Section Drawing of Total Radiation Calorimeter	43
30.	Temperature Rise in a Semi-Infinite Solid with Constant Heat Flux at the Boundary	44
31.	Tentative Calorimeter Design with Blocking Holes	45
32.	Heat Conduction Path for Calorimeter	45
33.	Temperature Rise as a Function of Path Width Ratio	47
34.	Temperature Rise as a Function of Incident Heat Flux	47

LIST OF SYMBOLS

B	Boltzmann's Constant
c	Velocity of Sound
d	Tube Diameter
d_1	Diameter of Transducer Membrane
D_1	Diameter of Tube Connecting Arc to Transducer
E	Electrical Gradient
f_n	Undamped Natural Frequency
I	Spectral Intensity
I_{max}	Maximum Value of I
$I'(x)$	Derivative of I(x) with Respect to x
ℓ_1	Height of Dead Volume Before Pressure Transducer
L_1	Distance from Arc to Transducer
n_o	Density of Radiating Particle in Ground State
p	Pressure
R	Radius of Tube Containing Arc
R_e	Reynolds Number
r	Radial Distance from Arc Axis
S	Radiation Rate Per Unit Volume
T	Absolute Temperature
T_{max}	Temperature of I_{max}
T_{Lam}	Temperature of Laminar Arc
T_{Turb}	Temperature of Turbulent Arc
v	Velocity
x	Cartesian Coordinate

LIST OF SYMBOLS (Cont'd)

y	Cartesian Coordinate
Z_o	Partition Function of Ground State
ΔT	Amplitude of Temperature Fluctuation
$\mathcal{K}$	Thermal Conductivity
$\mathcal{K}^*$	Effective Thermal Conductivity Produced by Turbulent Mixing
λ	Wavelength
μ	Dynamic Viscosity
ν	Kinematic Viscosity
φ	Excitation Energy
ρ	Density
σ	Electrical Conductivity
Ω	Electrical Resistance

ELECTRIC ARCS IN TURBULENT FLOWS III

1. INTRODUCTION

1.1 General Remarks

The problem of the turbulent and laminar flow modes has been of great interest for fluid dynamic studies at moderate temperatures. This is mainly because in the turbulent mode the transfer processes for energy, momentum and mass are strongly accellerated, up to a factor of 10 or even of 100.

The question arises therefore, whether turbulence is of similar importance at the substantially higher temperatures found in electrical arcs. Arc apparatus has been used in industry for a long time, (1, 2) and its use is presently expanding to a number of challenging new applications, (3, 4). The proper determination of the flow mode and the collection and correlation of energy, momentum and mass transfer data is of great importance for the design of this apparatus.

It must therefore be considered an unsatisfactory state of affairs that presently only a few initial investigations have been published on the flow mode of electrical arcs (5, 6, 7). This paper hopes to present some further progress in the direction of gaining a better understanding of the associated phenomena.

1.2 Estimate of Reynolds Numbers

A simple order of magnitude estimate of the Reynolds number of a plasma in a flow tube may help to recognize the importance of some of the parameters involved. For this estimate the plasma temperature shall be assumed to be constant over the tube diameter and viscosities will be taken from the theoretical work of Yos (8) for nitrogen, with densities from calculations of Burhorn and Wienecke (9). With these numbers one gets first the theoretical curves for the kinematic viscosity, $\nu = \frac{\mu}{\rho}$ of Figure 1. From these curves, upper limits for the kinematic viscosity can be taken in the temperature range up to 30,000° and with the additional values:

Tube diameter: $d = 1$ cm.
Flow velocity: $v = 2 \times 10^6$ cm/sec.

a lower limit for the Reynolds number $Re = v \cdot d \times \mu/\rho$ of a flowing nitrogen plasma can be calculated, for the pressures 1; 3; 10 and 30 atm. Thus one gets the values of Table I.

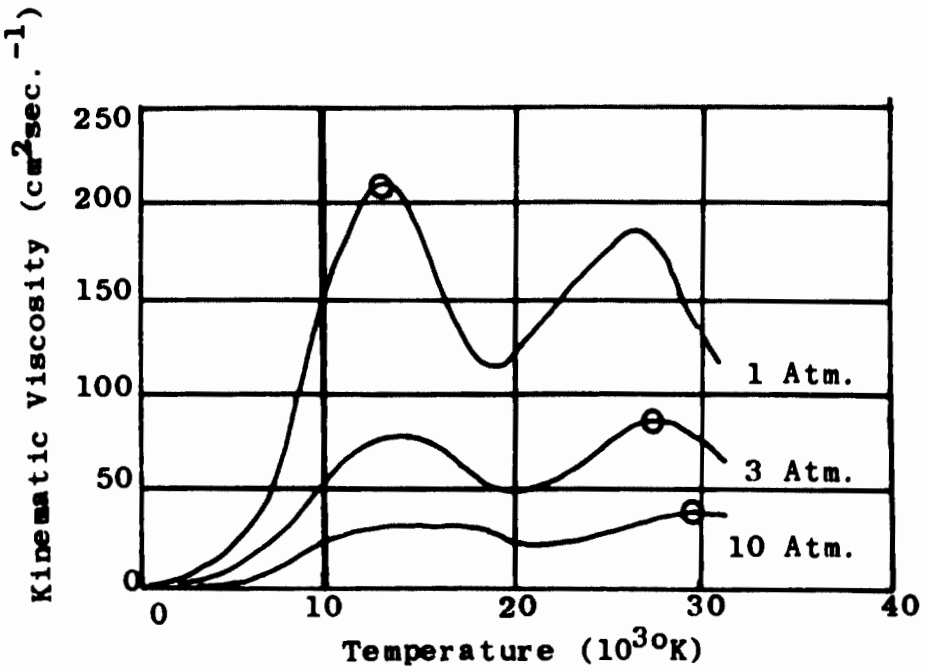

Figure 1 - Kinematic Viscosity of Nitrogen Plasma

0 0 These values were used for Estimate of Re-Number

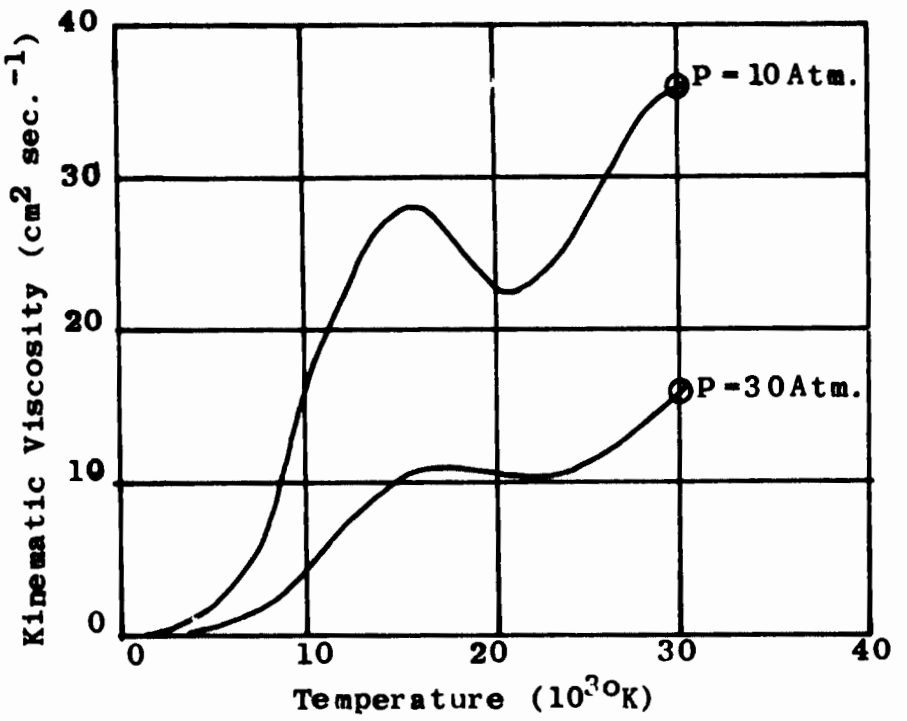

Figure 1a - Kinematic Viscosity of Nitrogen As a Function of Temperature

TABLE I

PRESSURE	ATM	1	3	10	30
RE-NUMBER	---	980	2450	5600	12,700

This table shows that turbulent effects must be expected in arcs for the conditions mentioned above if the pressure exceeds the value 3 atm. Because upper limits of viscosity were used and the effects of the colder outer parts of electrical arcs were disregarded in this estimate, turbulence can be expected at still lower pressures.

This result agrees reasonably well with observations in the literature. Runstadler (5) clearly found turbulence in high flow speed argon arcs burning in a tube of 1 cm diameter with currents up to 200 amps. The turbulent level in these experiments was weaker at high currents than at lower ones, which should be expected in view of the steep increase of viscosity with temperature, (Figure 2). Turbulent effects were found to be still much more pronounced at higher pressures, as shown in our earlier report (6) for argon arcs with pressures up to 10 atm., and currents up to 100 amps.

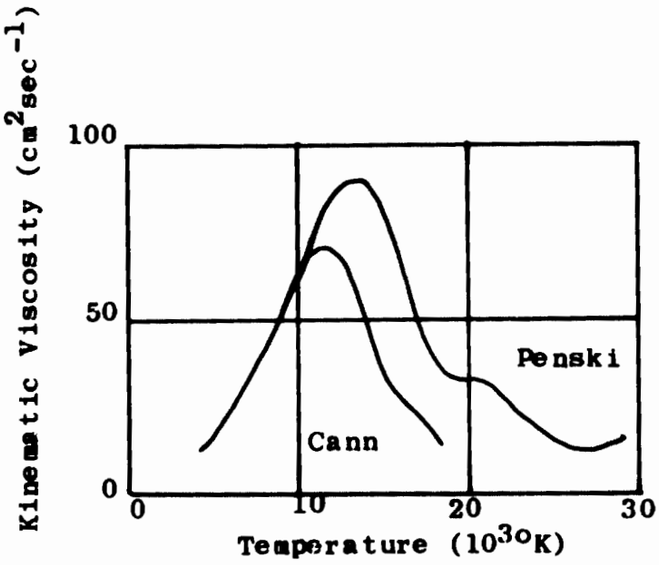

Figure 2 - Kinematic Viscosity of Argon
Ref. 10 and 11

2. IMPORTANCE OF FULLY DEVELOPED FLOW AND DEFINITION OF GOAL OF THIS INVESTIGATION

2.1 Fully Developed Flow

The equations for the transfer of energy, momentum and mass are very complex in the general case of a flowing fluid (12). If one wants to study one particular aspect of this general situation, namely the turbulent one, it is therefore advisable to conduct this study first under conditions of less complexity. Such a case, which is also of considerable practical importance, is the arc in a cylindrically symmetric tube and particularly in the so-called fully developed flow area of that tube, (Figure 3). In the fully developed flow area of a cylindrical tube the flow terms, convection, and expansion can be approximately neglected (5, 6), and the following relatively simple energy balance can be used for a stationary arc:

$$\sigma E^2 + \nabla\kappa\nabla T + \nabla\kappa^*\nabla T - S(T,p) = 0^*$$

Input Laminar Turbulent Radiation

* A list of the symbols is given at the beginning of the text.

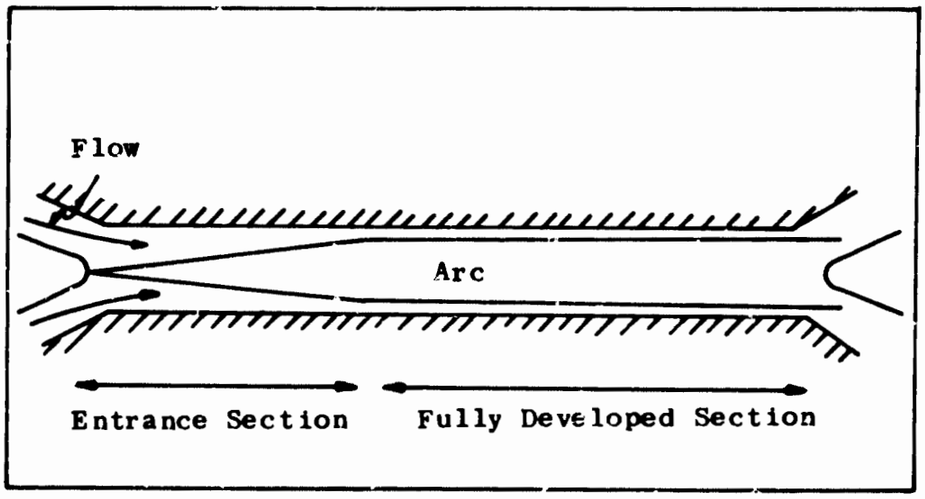

Figure 3 - Development of an Arc in Coaxial Flow, Schematic Drawing

In this equation we still find terms for the electrical input, for laminar and turbulent thermal conduction and for radiation. The equation has only one term, the turbulent one, which does not occur in the well investigated Elenbaas equation (13, 14, 15). The bulk of information gained for the Elenbaas equation can therefore serve as a starting basis for turbulent studies.

In previous work with turbulent arcs we have started from that basis and it may be useful to recall some of the results obtained then (6):

a) Region of fully developed conditions was found in the portion of the arc at the end of the long flow tube.

b) The turbulent energy loss term at conditions of high "Re" numbers in the fully developed flow area was considerably larger than the laminar term.

c) The turbulence of the high flow rate plasma was directly confirmed by $\mu\mu$c photography.

d) It was qualitatively found that the turbulent level increased with an increase in Reynolds number.

2.2 Goal of Investigation

The results obtained last year suggest strongly that one should search for a possible quantitative relationship between turbulent heat transfer and Reynolds number and/or other non-dimensional parameters of the flow and temperature field. Such a study requires, besides other measurements, the determination of the arc temperature and of the velocity in the arc, which, for a turbulent arc, have not yet been attained.

The main goal of the first part of this investigation is therefore to study methods suitable for a definition of the temperature and flow field of a fully developed turbulent arc, and then to apply them for measurements. Other goals include an extension of the important parameters, current and pressure, to higher values than reached earlier (6), and also to experiment with nitrogen plasma in addition to argon. It is hoped that with these goals accomplished, in a second part of this work, an experimental correlation can be found between radial turbulent heat transfer and non-dimensional quantities of the flow field.

3. APPARATUS

The basic experimental arrangement has not changed since the last report, (6). We utilize the thermal storage capability of rectifiers, resistors, and cascade discs to withstand transient heating. The uncooled copper discs have withstood heat fluxes of 13Kw/cm^2 for short periods. Transient operation ($\sim$ 0.5 sec.) makes it necessary to record data with CRT oscilloscopes. Gas flow is metered by critical orifices whose upstream pressure is kept at three times the tube pressure. Orifices were calibrated with an absolute accuracy of $\pm$ 10%; relative accuracy is $\pm$ 2%. Because of the extremely high potential gradients produced by turbulent nitrogen, cascade discs were made of 0.5mm thick copper; for experiments in argon 1mm discs were retained. Preparation of the discs included cleaning in an ultrasonic bath and etching a 0.02mm deep layer from the surface. This process insured cleanliness and removed the sharp edges which increase the chances for "strike over" at the walls. The discs were insulated by 0.25mm thick teflon washers which were recessed from the arc to prevent contamination. Before experiments, the discs were carefully aligned with a steel rod whose diameter matched the 7mm I.D. of the discs.

Modifications of the tube include a new cathode holder which reduces the dead volume between the critical orifice and the cathode, and a simplified connecting arrangement so the tube can be attached to the electrical and flow systems quickly without using bolts. Figure 4 shows a tube made up for spectral studies; other special purpose tubes were made for voltage gradients, pressure gradients, and plasma photography. These are described below in their respective experimental sections.

The optical apparatus is described under section 4.412 Spectroscopic Instrumentation.

Figure 4 - Cascade arc constrictor with window for spectral observation. Similar tubes have been made for other special purposes: measurement of potential and pressure gradients, and for high speed photography. Anode-Cathode distance is 50cm, arc tube diameter is 0.7cm, ratio is 71:1.

4. EXPERIMENTS

4.1 Measurements of Potential Gradient

4.11 Methods

Previous researchers have discussed the importance of the arc voltage characteristic as a means of gaining insight into the energy transfer process of electrical arcs (14).

The situation is especially simple in a longitudinal flow arc if "fully developed conditions" are reached. In this regime the value of the electrical gradient is a direct measure of the intensity of the radial heat transfer.

Earlier, (6), we had found that a ten atmosphere argon arc exhibited a considerably higher electrical gradient at a high flow rate. This result, which covered the region from 0.23 to 2.95 grams/sec. and from 10 to 100 amperes in a 0.5cm diameter tube, could be interpreted as a consequence of turbulent as opposed to laminar heat transfer. It was clear, however, that the difference between the turbulent and laminar electrical gradients diminished with increasing current. Extrapolation of the arc characteristic suggested that any significant difference between the high and low flow rates might disappear in the vicinity of 200 amperes. Such a merger of characteristics would be understandable from a theoretical viewpoint based on the temperature dependence of argon viscosity (Figure 2). At higher temperatures the effective kinematic viscosity ν rises, so that arcs of larger currents might have lower effective Reynolds numbers. Of course, this diminished Reynolds number can finally fall below the critical point under which turbulence cannot subsist. In view of this situation we used a slightly larger tube diameter (7mm instead of 5mm) for the experiments reported here.

Potential gradients were measured by attaching resistive dividers ($6 \times 10^6\ \Omega$ input impedance) to eight cascade discs spaced along the arc tube. A typical current drawn from the plasma region would be 3×10^{-5} amperes. Data was necessarily recorded as cathode ray oscilloscope traces.

4.12 Results

A constant voltage gradient was found in all experiments with argon; a deviation occurred in nitrogen at high flow rates and low currents. Under these conditions the graph breaks into two linear regions each occupying half the tube. Figure 5 shows the most extreme case encountered - twenty-six amperes in a flow of 6.5 grams/sec. As the current increases the two slopes approach the same value until 130 amperes where the two merge. This increase in the potential gradients in the second half of the tube is not explained, but it is felt that the value in the fully developed region should be taken as correct.

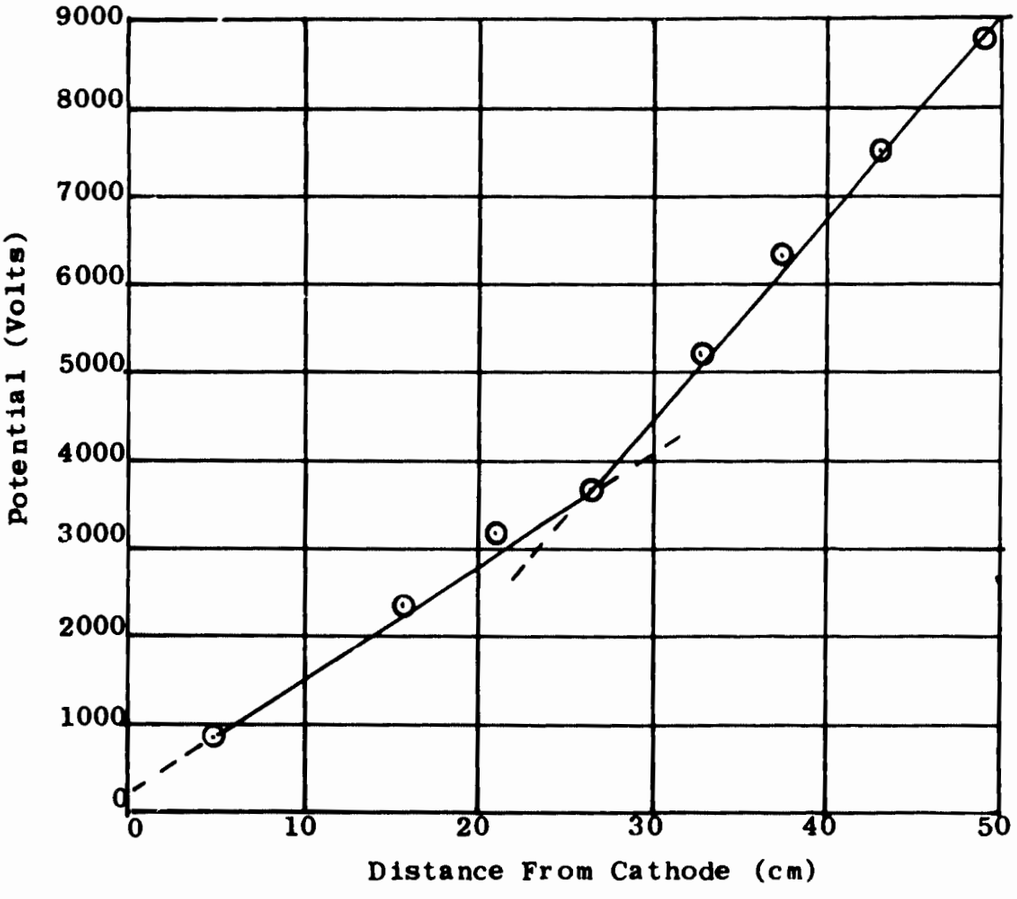

Figure 5 - Potential Along Length of Arc Constrictor

Tube Diameter:	0.7 cm
Tube Length:	50 cm
Gas:	Nitrogen
Current:	26 Amps.
Flow Rate:	6.5 gr/sec.

With this interpretation, the arc characteristic is shown for argon and nitrogen in Figures 6 and 7. The dramatic influence of flow rate is indicated by the wide separation of the low and high flow cases. Voltage gradients significantly higher than the ones displayed here can be produced by further increasing the gas flow. This was not done here so that the effect of a significant pressure drop along the arc constrictor could be avoided. Note that, although the same orifice was used for argon and nitrogen, the flow rates are altered by the different gas densities.

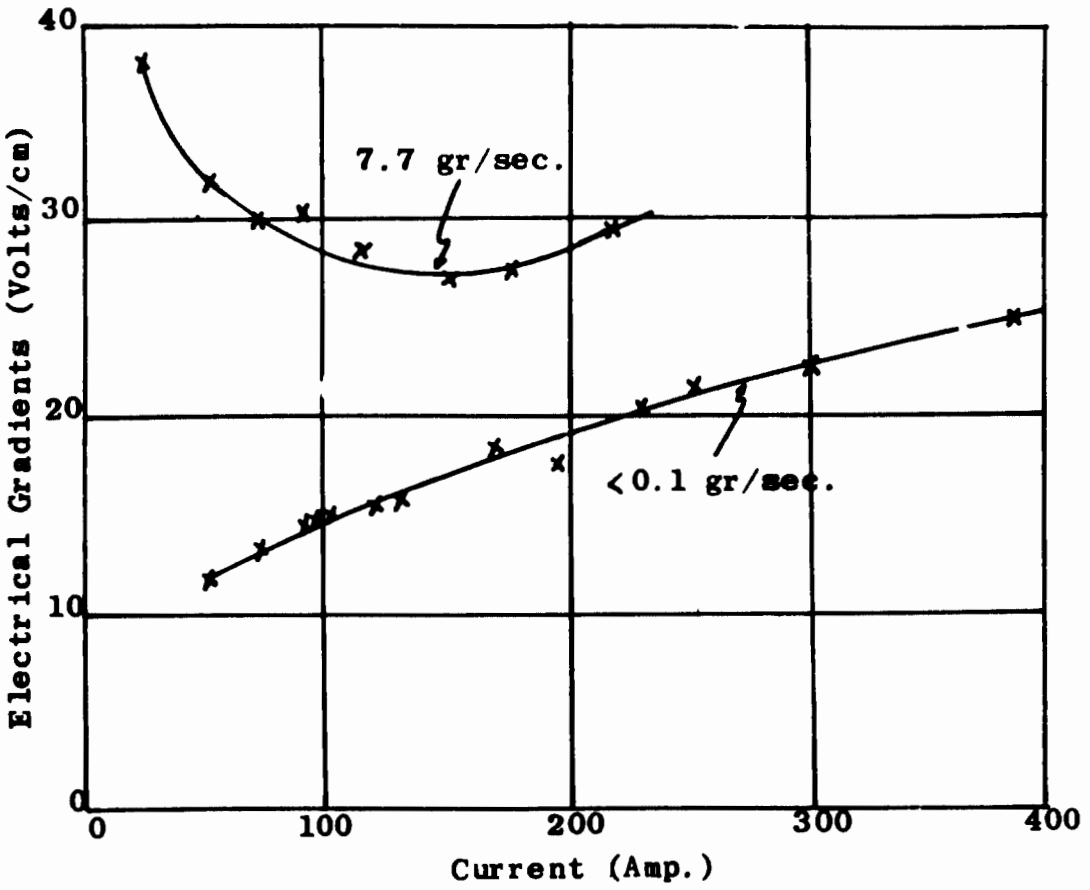

Figure 6 - Characteristics of Argon Arcs at 11.2 Atm.

Tube Diameter:	0.7 cm
Tube Length:	50 cm
Gas:	Argon
Pressure:	11.2 Atm.
Flow Rates:	<0.1 gr/sec.
	7.7 gr/sec.

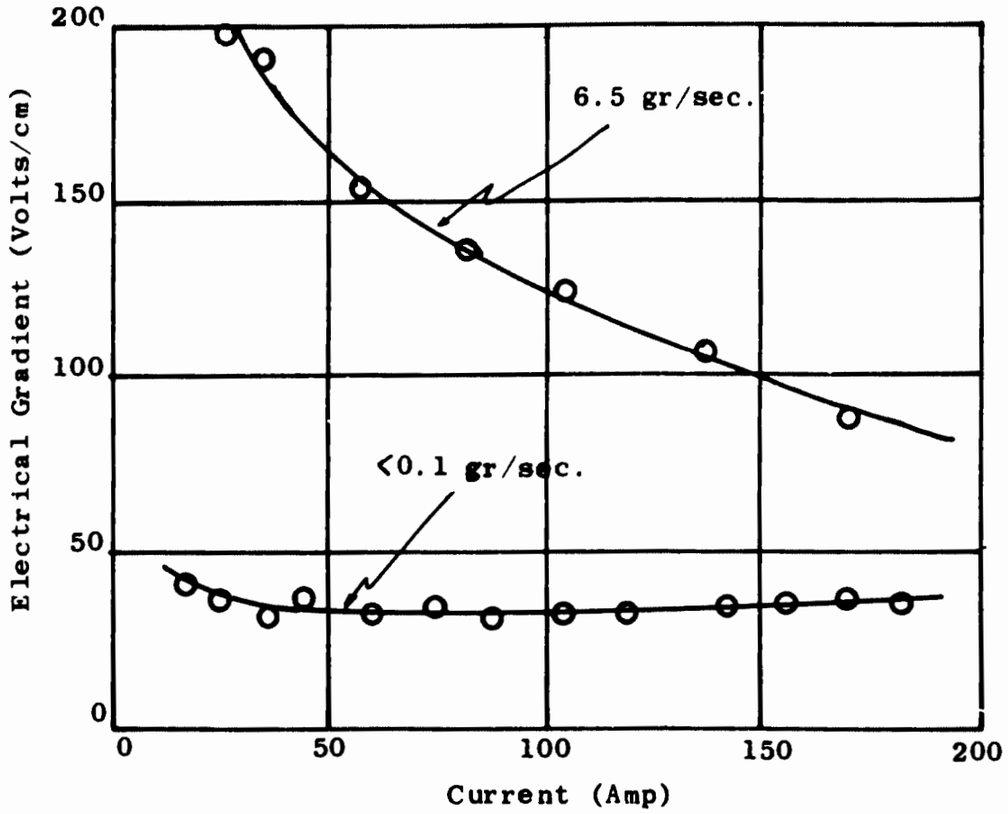

Figure 7 - Characteristics of Nitrogen Arcs at 11.2 Atm. Pressure

Tube Diameter:	0.7 cm
Tube Length:	50 cm
Gas:	Nitrogen
Pressure:	11.2 Atm.
Flow Rates:	6.5 gr/sec.
	<0.1 gr/sec.

4.2 Measurement of Pressure Gradient

4.21 Methods

The efficiency of pressure gradient measurements in providing a revealing characterization of the flow mode in a cylindrical arc was shown by Runstadler's plot of friction factor versus Re-number, (5). His graph shows a break from the linear relationship of laminar flow in one atmosphere argon.

It was felt quite desirable to extend these measurements since the effect reported by Runstadler disappeared at higher currents and since there was some doubt that a significant portion of the arc was fully developed at the highest flow rates.

Local pressure in the arc constrictor was read by connecting a quartz pressure transducer to the high pressure region through a long but narrow tube (Figures 8 & 9). The quartz transducer is connected to a high input impedance charge amplifier whose output is registered on a cathode ray oscilloscope. Five of these assemblies were placed along the arc so it was possible to determine pressures simultaneously and thus to measure the pressure gradients.

The transducer was far removed from the arc because of the several thousand volt potential associated with the anode region. The recording oscilloscopes which are electrically connected with the transducers must be maintained at ground potential and thus offer a possible "strike-over" point to the arc. As further protection, neon discharge bulbs were placed between the transducer housing and ground. This bulb acts as an open switch until ~ 75 volts appears across the contacts; it then freely breaks down and, as tests proved, can carry several hundred amperes for a short period with only a 70 volt potential drop.

The remoteness of the quartz transducer from the arc constrictor necessitates a close look into the influence this has on the pressure readings. Treating our design as a second order, lumped constant system, the following undamped natural frequency has been derived (16):

$$f_n \approx \frac{C}{2\pi L_1}\left[\left(\frac{d_1}{D_1}\right)^2 \frac{\ell_1}{L_1} + 1\right]^{-1/2}$$

For our case the values are: $L_1 = 15$ cm.; $d_1 = 0.5$ cm.; $D_1 = 0.06$ cm. $\ell_1 = 0.02$ cm. Taking a value of 350 msec. for the average velocity of sound in the passage tube gives $f_n \approx 290 H_Z$. This checks roughly with the oscillograph traces which showed $100 H_Z$ fluctuations and a rapid response to the fuse wire explosion at initiation of arcing. The pressure gauge itself (Kistler Model #601A) is rated for a $10{,}000 H_Z$ response.

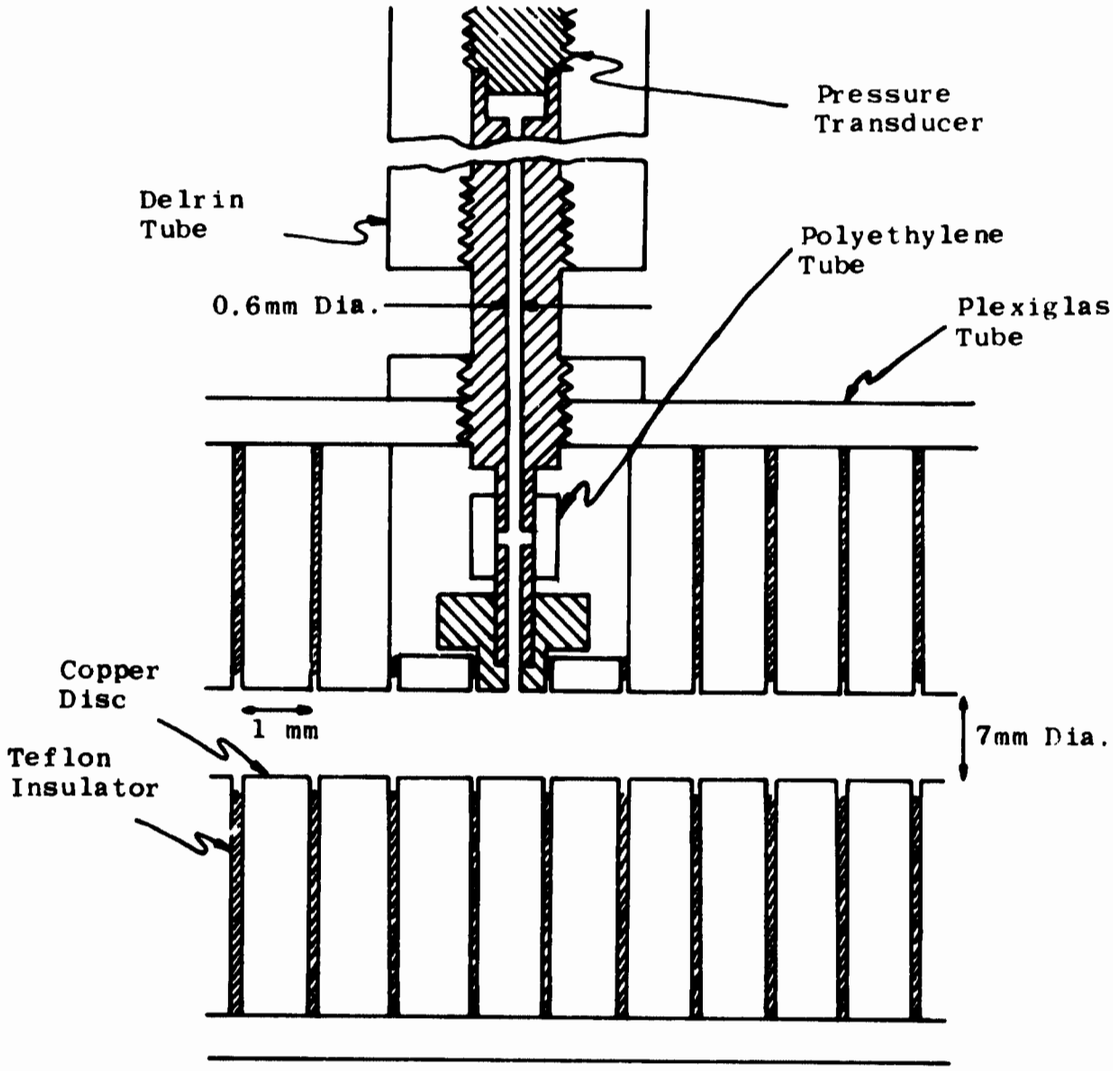

Figure 8 - Pressure Tap, Schematic Drawing

Note, That Drawing is Not to Scale
The 0.6mm Diameter Duct From Arc
to Transducer is 15cm long.

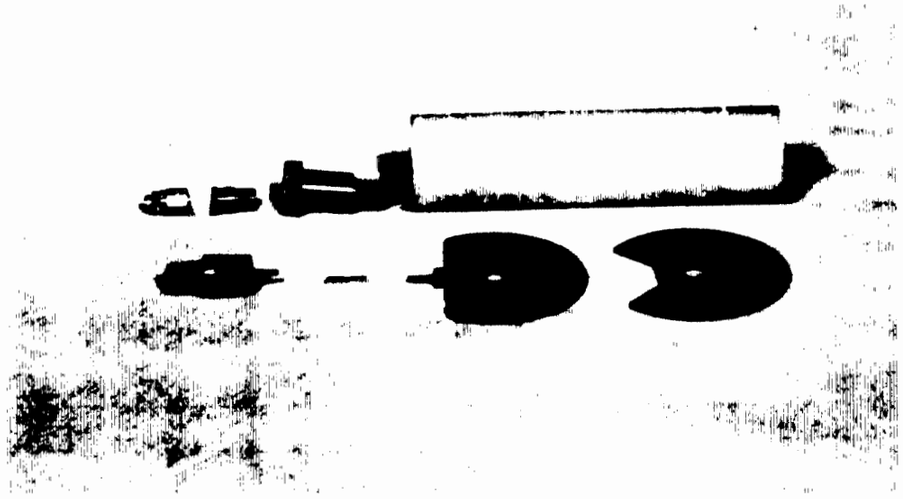

Figure 9 - Components of Pressure Tap

Pressure transducer at upper left fits into a holder-adapter which screws into long delrin rod which serves to insulate the measuring system from the arc. The adapter at bottom left connects the delrin rod to the pressure tap disc by means of a short length of polyethylene tubing. The pressure tap disc is 1mm thick and contains a drill hole leading into the 7mm arc constrictor bore. The disc at right must be stacked beside the pressure tap disc.

4.22 Results

A typical plot of pressure change versus distance from the cathode, which was at the upstream end of the tube, is shown in Figure 10. All measured pressure drops are linear to the accuracy of our measurements. Measurement is made after one half second of arcing so the pressure in the downstream reservoir has risen measurably from the addition of hot gases. In the case shown, this amounts to an increase of 2.1×10^4 dynes/cm^2 or 0.3 psi, which can be seen as the pressure increase at the end of our 50cm long cascade. The accuracy of the measurement can be inferred from the stray of the points; the accuracy of the gradient should be better because of averaging the five points.

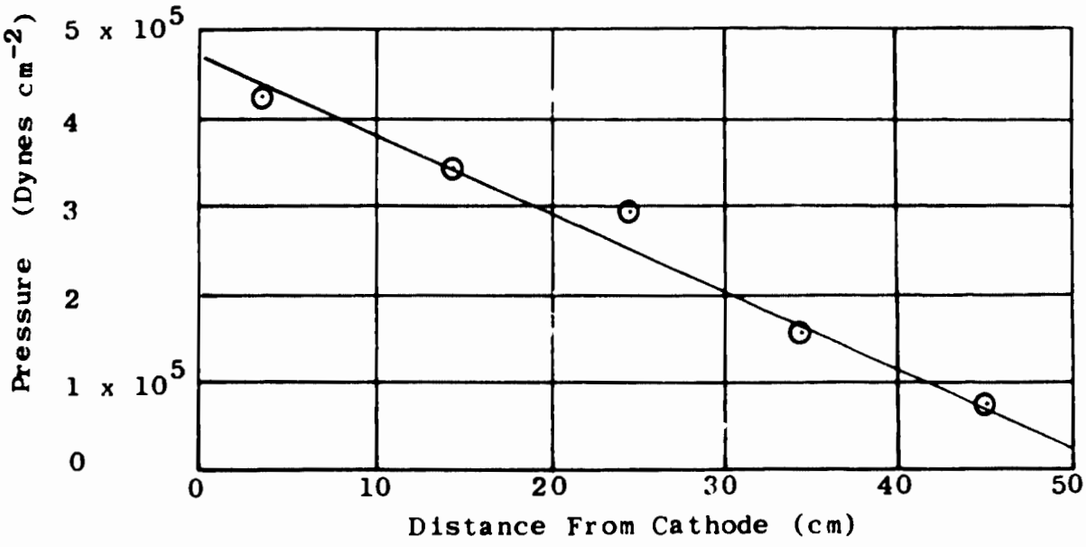

Figure 10 - Pressure Along Cylindrical Argon Arc

Tube Diameter:	7 mm
Gas:	Argon
Pressure:	11.2 Atm.
Current:	122 Amperes
Flow Rate:	5.2 grams/sec.
Pressure Gradient:	9.0 x 10^3 Dynes/cm^3
Test #:	275

Figure 11 shows the dependence of pressure gradient on arc current in argon with flow rate held constant. There is surprisingly little variation at higher currents, a fact which is utilized in the next series of tests.

Holding current constant at 125 ± 4 amperes and changing the flow rate produces the results of Figure 12. The log-log plot covering the range 2 grams/sec. - 14 grams/sec. shows a 1.8 power dependence of pressure gradient on flow rate. This is just about the same dependence found in cold turbulent flows (17), whereas a linear relationship holds in laminar flows. The result in Figure 12 is therefore significant evidence for the existence of turbulence in our arc tube. Note too, in Figure 12, that turbulence apparently exists at the moderate flow rate of 2 grams/sec., well below the level chosen for the "turbulent" experiments of this report.

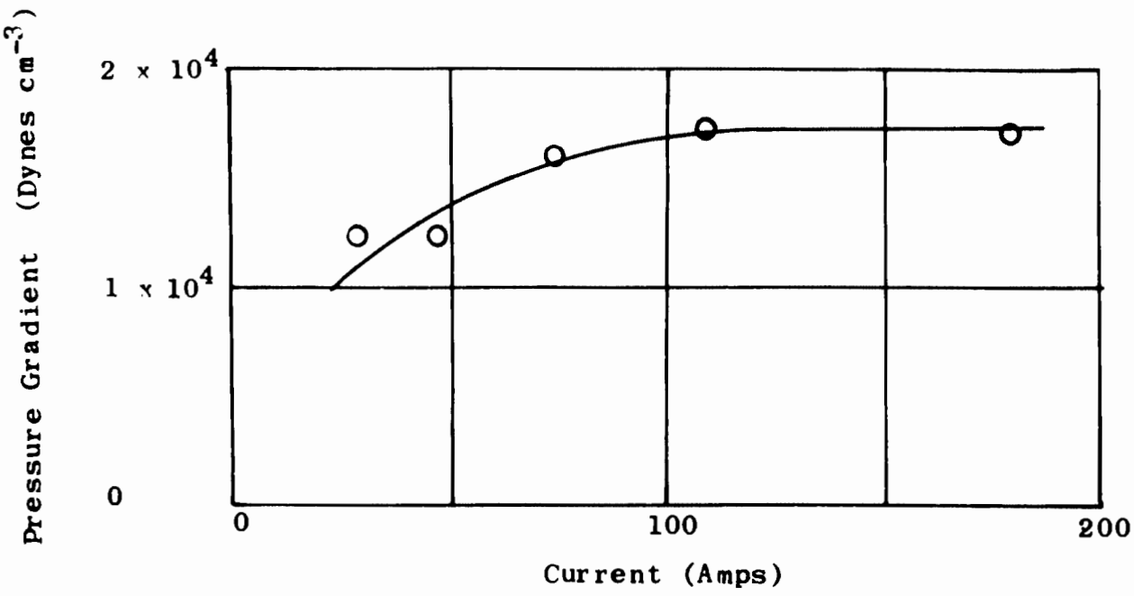

Figure 11 - Dependence of Pressure Gradient On Arc Current

Tube Diameter: 7 mm
Gas: Argon
Pressure: 11.2 Atm.
Flow Rate: 7.7 grams/sec.

These pressure gradient measurements as yet, have been made in argon only. The high voltage gradients associated with turbulent nitrogen flow require copper cascade discs of 0.5mm thickness to prevent arc-over at the tube wall and this disc is too thin for the 0.6mm diameter drill hole which connects the pressure transducer with the arc tube. Measurements of nitrogen pressures will require design of a suitable insulating disc to contain the drill hole.

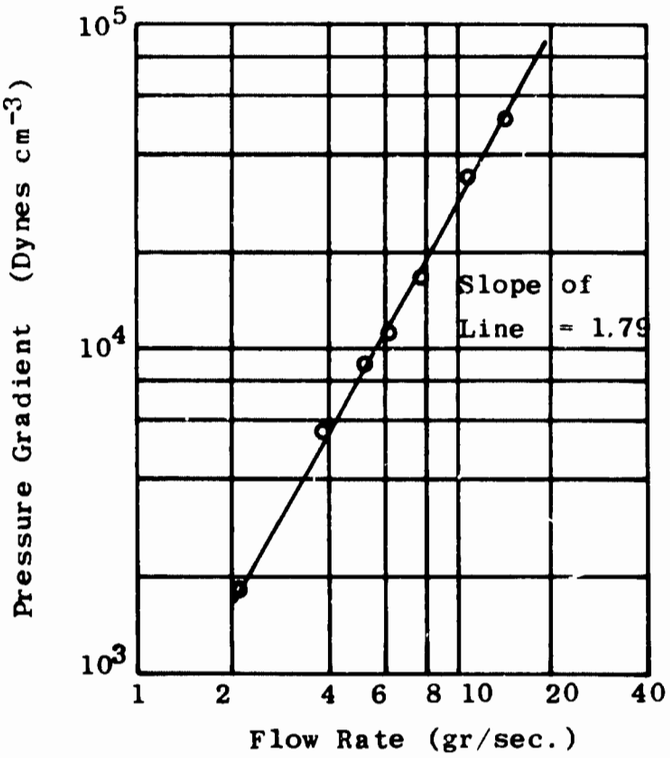

Figure 12 - Dependence of Pressure Gradient on Flow Rate, Turbulent Regime

Tube Diameter:	0.7 cm
Tube Length:	50 cm
Gas:	Argon
Current:	125 + 4 Amp.
Pressure:	11.2 Atm.

4.3 Measurements of Plasma Velocity

4.31 Methods

The importance of velocity measurements lies in the necessity of establishing a definition of a Reynolds number for the hot plasma stream and also investigating the relationship of heat transfer to other dimensionless parameters. Obviously, then, it is of fundamental importance to know the relationship between velocity and the major variable parameters of the arc, such as current, flow rate, etc.

Plasma velocities were determined by short time sequential photography of a section of arc observed through a quartz tube which replaced a 14mm long section of the copper cascade. Movement of the natural turbulent plasma structure between the two exposures was measured to give plasma velocities near the center of the arc.

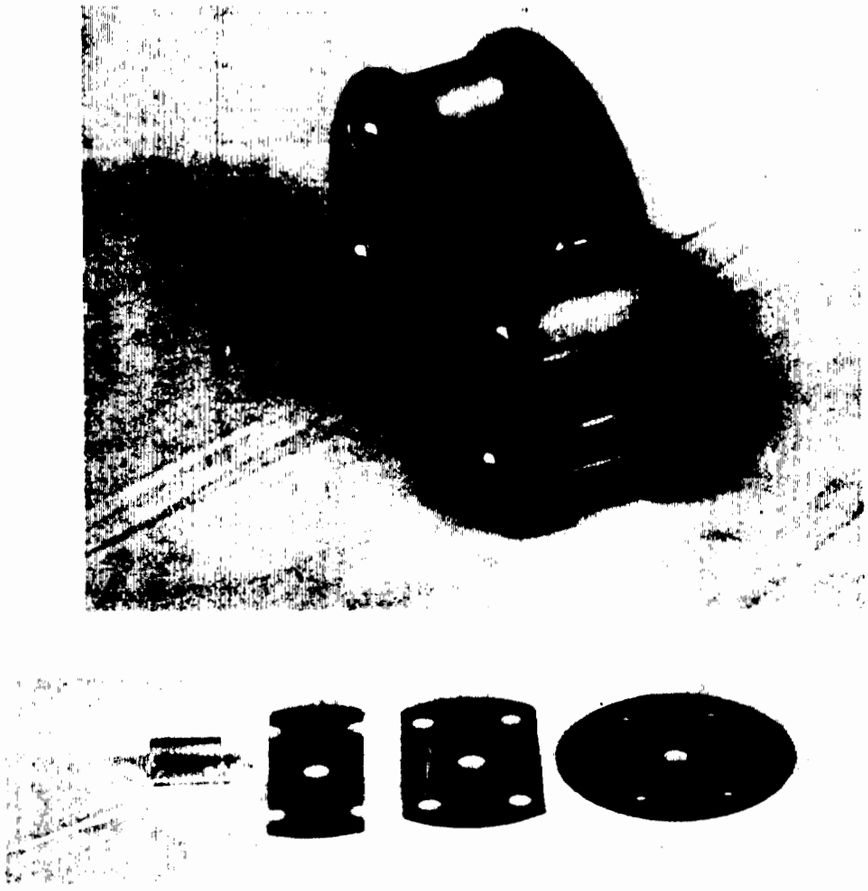

Figure 13 - Quartz Window used for Photographic Determination of Plasma Velocity

Above: Completed Assembly
Below: Quartz Tube and Copper Discs

The quartz is clamped between copper discs which are spaced by insulators.

The quartz "window" was a tube with a 7mm inner diameter, to match the normal constrictor dimension, and a 1mm thick wall. The seal at the ends was made by pressure from the four screws, (Figure 13). The joint was judged to be rather tight considering that the window was placed near the anode end of the tube where no more than 2 psi pressure increase is expected. The curved shape of the "window" inevitably distorts the view of the interior with an effect which grows as the walls are approached. The photographs presented here, however, are of near axial objects and it must be kept in mind that a design more optimal from the optical viewpoint could produce misleading disturbances of the arc which might be interpreted as naturally occurring turbulence.

The camera used was a Beckman and Whitley dual frame image converter camera with two model 525XL camera heads and a model 5062 beam splitter. The specifications of the camera tube (IC25) include a resolution of 22 lines/mm and a 40 times image intensification at 4,400Å.

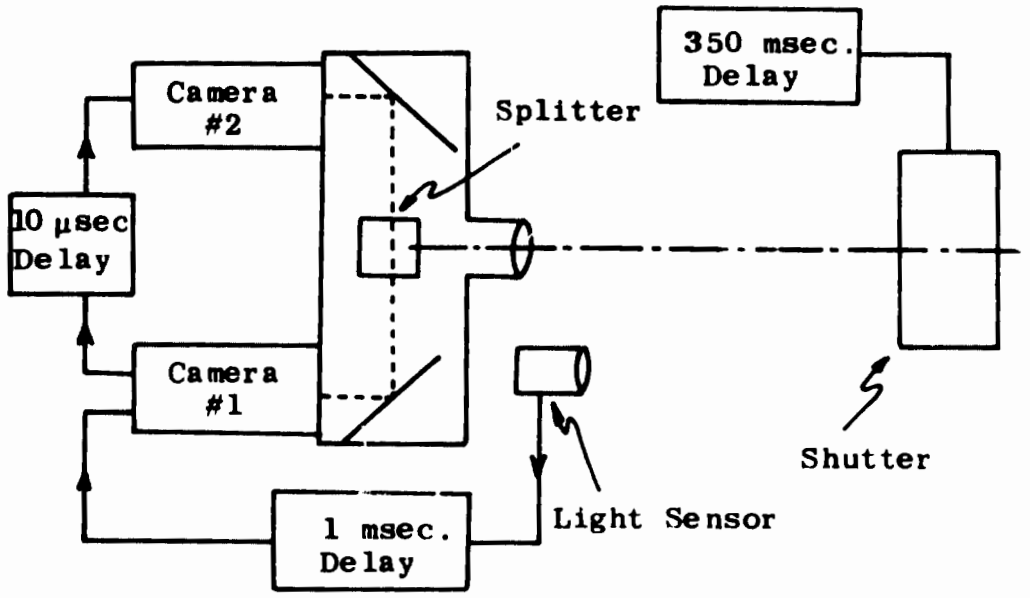

Figure 14 - Electronic Operation of Image Converter Camera System, Block Diagram

Short exposures are produced by operating the camera's picture tube with a power pulse of variable duration. When unpowered the tube acts as a closed shutter; when powered as a view screen. A small fraction ($\approx 1 \times 10^{-6}$) of the incident light does leak through the tube even when no power is applied, so a mechanical shutter is required to reduce the time integrated ratio of "leakage" light to "exposure" light. To accomplish this a compur shutter was placed in front of the window and the cameras triggered by a light sensor which detected the opening of the shutter (see block diagram Figure 14). This operation requires three delay units; the first allows the arc 350 msec. to develop into a steady state condition; the second delay of 1 msec. insures that the shutter has opened fully before the cameras photograph the arc; the third spaces the two tubes of the camera so that velocity can be determined. The flexibility of this third delay (continuously variable range of 100 nanoseconds to several milliseconds) is a substantial, and necessary, improvement over the framing camera used for the last report.*

The photographs of Figures 15 and 16 were taken with the mechanical shutter open for 5 msec., the image converter tube powered for 1 μsec., and the lenses adjusted for a magnification of 1.2 x full scale. Motion of the turbulent structures was measured using the edge of the window as a reference point.

4.32 Results of Velocity Measurements

It is immediately seen from the photographs that turbulent structure exists on a scale much smaller than the tube diameter. This turbulent structure appears to disturb the entire plasma region, not just the outer layers. The top four photographs in Figure 15 also show that photographic light intensity decreases with flow rate. It should be mentioned, however, that the strong development of these films results in a "hard" response to light i.e. variations in exposure are magnified by the film. It is interesting to compare this result, found in argon, with the decreased intensity found in the turbulent nitrogen arc and reported in Section 4.433 of Temperature Measurements.

* Dynafax Model 326 of Beckman and Whitley, Mountainview, California.

Flow Rate: 5.2 grams/sec.
Current: 102 Amp.
Test #: 251

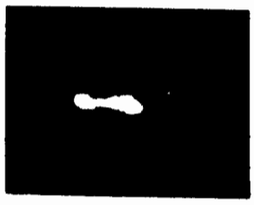

Flow Rate: 6.1 grams/sec.
Current: 100 Amp.
Test #: 258

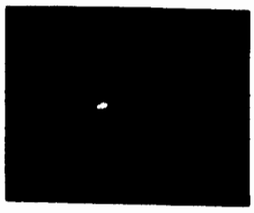

Flow Rate: 7.7 grams/sec.
Current: 100 Amp.
Test #: 247

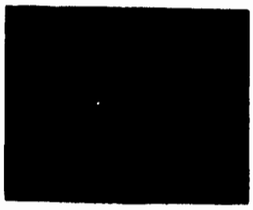

Flow Rate: 10.8 grams/sec.
Current: 96 Amp.
Test #: 254

Flow ⟶

Figure 15-Image Converter Photographs of Argon Arcs Showing the Influence of Flow Rate

Tube Diameter:	0.7 cm
Tube Length:	50 cm
Length to Window:	43 cm
Gas:	Argon
Pressure:	11.2 Atm.
Exposure:	1 μsec.
Magnification:	1.2 x full scale

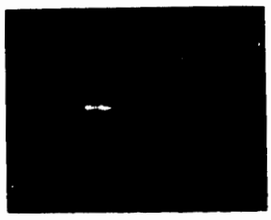

First Exposure

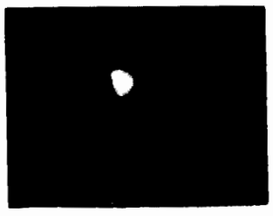

Second Exposure - Delayed 8μsec.

Figure 16 - Sequential Image Converter Photographs of a Turbulent Argon Arc. The Apparently Lower Intensity of the Second Photograph is due to an Inbalance of the Two Picture Tubes.

Tube Diameter:	0.7 cm
Tube Length:	50 cm
Length to Window:	43 cm
Current:	86 Amp
Flow Rate:	7.7 gr/sec.
Gas:	Argon
Pressure:	11.2 Atm.
Exposure:	1 μsec.
Magnification:	1.2 x full scale
Test #:	259

When the plasma velocity is plotted versus current (Figure 17) with flow rate held constant (at 7.7 grams/sec.) it is clear that current does not strongly influence velocity beyond a certain range. This initial range may correspond to a state in which the arc does not "fill" the tube well.

Figure 18 shows the important result that plasma velocity is linear with flow rate and apparently directly proportional to it. The apparent accuracy of the graph points, however, is misleading. At this time velocity must be considered accurate only within ± 20%.

One of the severe problems limiting accuracy is the evolution of plasma structures with time. The delay between exposures in our measurements, could not be increased indefinitely for the purpose of getting larger displacements of the plasma globuli because the fine details necessary for a precision measurement became distorted. This problem can be seen in the two photographs of Figure 16 which are separated by an 8 μsec. delay. Other photographs with longer delays between exposures, show that still more of the smaller structures have vanished. This unavoidable problem does, however, indicate the important fact that a vigorous mixing action occurs and that it penetrates to the core of the arc.

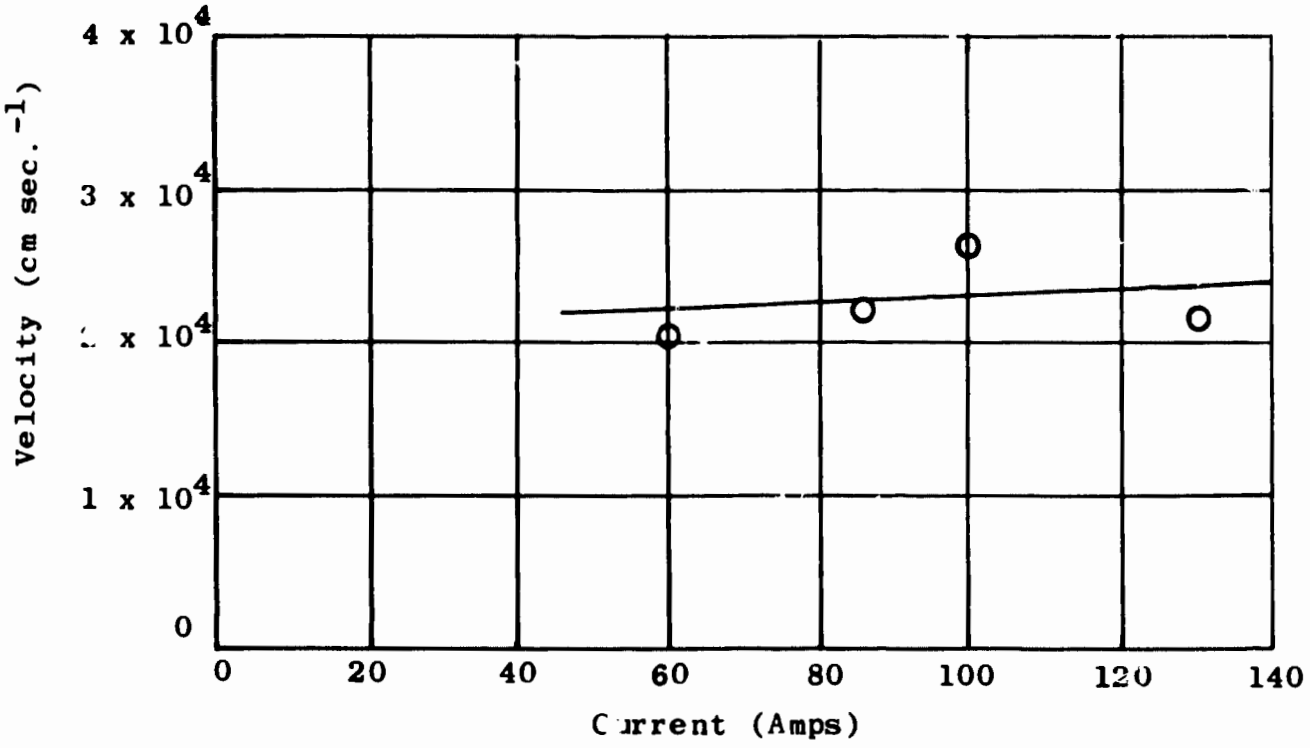

Figure 17 - Plasma Velocity as a Function of Arc Current

Tube Diameter:	0.7 cm
Tube Length:	50 cm
Length to Window:	43 cm
Gas:	Argon
Pressure:	11.2 Atm.

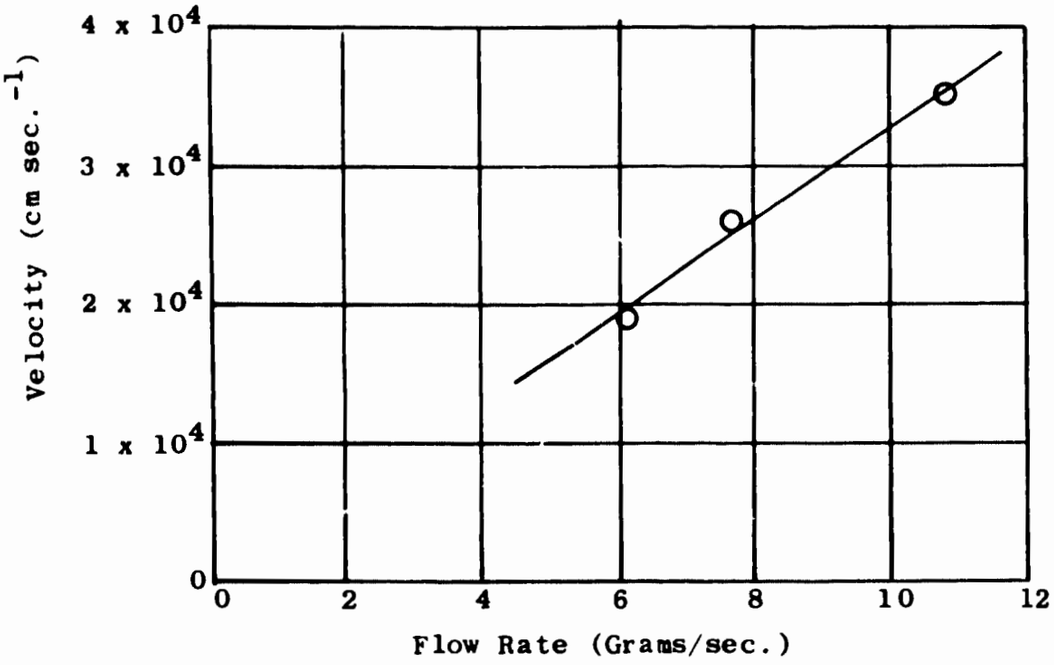

Figure 18 - Plasma Velocity as a Function of Flow Rate

Tube Diameter:	0.7 cm
Tube Length:	50 cm
Length to Window:	43 cm
Current:	100 ± 4 Amps
Gas:	Argon
Pressure:	11.2 Atm.

4.4 Measurements of Arc Temperature

4.41 Methods

4.411 Effect of Intensity Fluctuations on Measurement of Average Temperature

The special difficulty of a temperature measurement in a turbulent plasma lies in the fact that such a plasma has simultaneously random spatial and time fluctuations of all important values, such as temperature, velocity, pressure, etc.

These fluctuations destroy at any time moment cylindrical symmetry, a result which is particularly regretable because most of the evaluation methods for spectroscopic measurements, especially the well known "Abel" technique, depend on radial symmetry and can, therefore, not be used any longer for momentary measurements. However, if one extends the measurements over longer time durations, radially symmetrical average values are again found for temperature, radiation, etc. and it is therefore these average values which we will attempt to measure in this work.

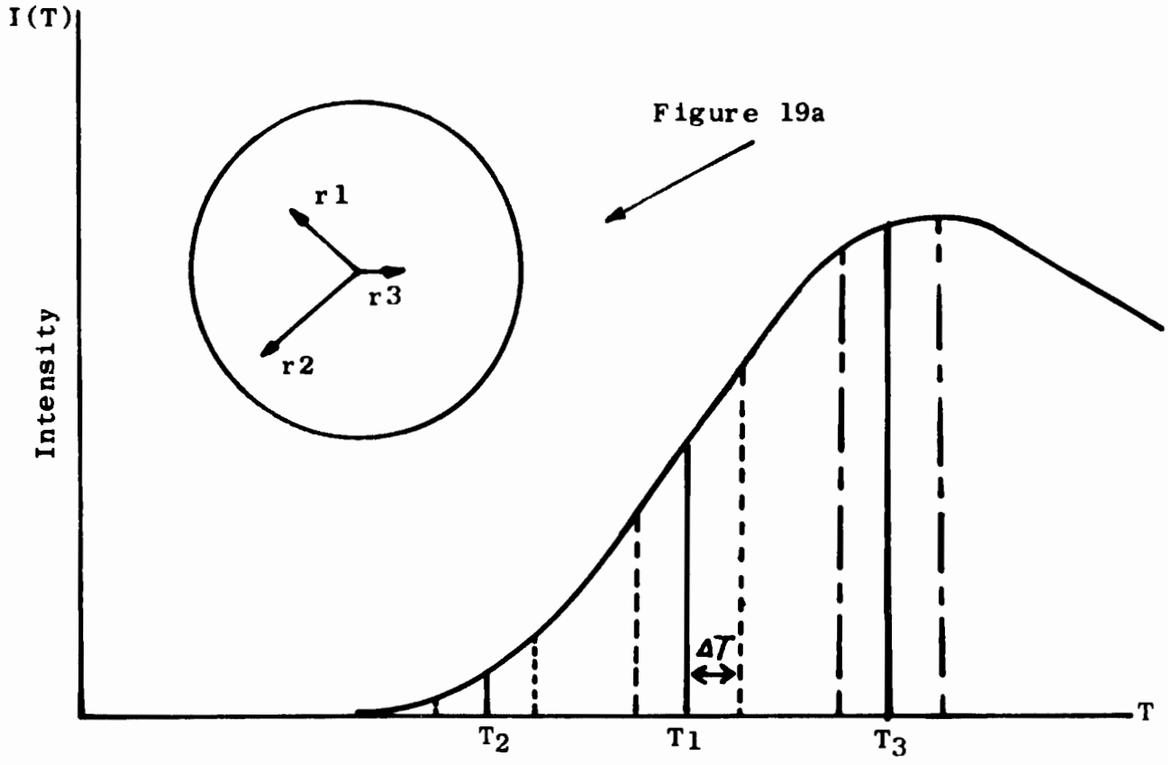

Figure 19 - Spectral Intensity as a Function of Temperature, Schematic

There is, of course, the question whether spectroscopic measurements lead to meaningful results in turbulent plasmas even in the case of a measurement of time average values, and we will address this question in the following section. To start out let us assume that the brightness of a spectral line in a turbulent arc as a function of the temperature is given by the schematic Figure 19. Let us assume further, that the brightness in point r_1, (Figure 19a) of the cylindrical arc corresponds to a temperature T_1. If, in addition, the temperature fluctuations in point r_1 are of modest amplitude and can be characterised by ΔT, the average brightness of the spectral line in this particular point will be practically of the same size with or without fluctuations, because I(T) is linear with T in the neighborhood of T_1.

If, however, the point r_1 has a lower temperature T_2, it is seen from Figure 19 that the average brightness in this case will <u>not</u> be the same as in the corresponding, not fluctuating case, but <u>higher</u> than that value.

The opposite effect occurs at point r_2. Here the average brightness of a fluctuating plasma will be lower than that of a laminar arc of equal "average" temperature.

It can therefore be stated qualitatively, that fluctuations will cause too high a value for brightness I(r) in a stronger than linearly rising part of the curve I(T), and too low a value in that part which is rising weaker than linearly. The correct I(r) value is only obtained at, or close to, the inflection point of the I(T) curve. This result has an important consequence. The local brightness I(T) can sometimes be measured directly in axial, or "end on" observation in a cylindrically symmetrical plasma. Therefore, if one selects in such a measurement spectral lines with suitable inflection points of their I(T) curve, correct average temperatures can be measured even in turbulent plasmas. The only additional condition in this case is: that the fluctuations ΔT are not too strong.

However, in many cases, and also in our own work here, "end on" observation is not possible and "side on" observation has to be used. In this case the quantity I(r) is not measured directly, but one measures the integral quantity

$$I(x) = \int_{-y_4}^{+y_4} I(r)\,dy$$

along a path of light through the cylindrical radiator as indicated by Figure 20. In this case one has no possibility of collecting light only from a certain axial distance r; but light from an extended area with a whole range of temperatures

has to be accepted. If we now assume that the highest temperature on beam X_4 is T_4 (Figure 20) then that part of the light coming from temperature range T_4 to T_5 will have nearly the correct intensity, at least for moderate turbulent fluctuations. However, the light coming from the areas with temperatures lower than T_5 will be more intense than its laminar equivalent.* In summation, then, light on beam X_4 will be somewhat more intense than it would be in the equivalent "laminar" case. The additional amount of light will be small only if the point T_5 is chosen high enough on the I(T) curve and particularly if the turbulent fluctuations are of small amplitude. From this discussion it is clear, that if the "error" on beam X_4 cannot be neglected, (Figure 20) it will be larger on beam X_6, further outside in the discharge.

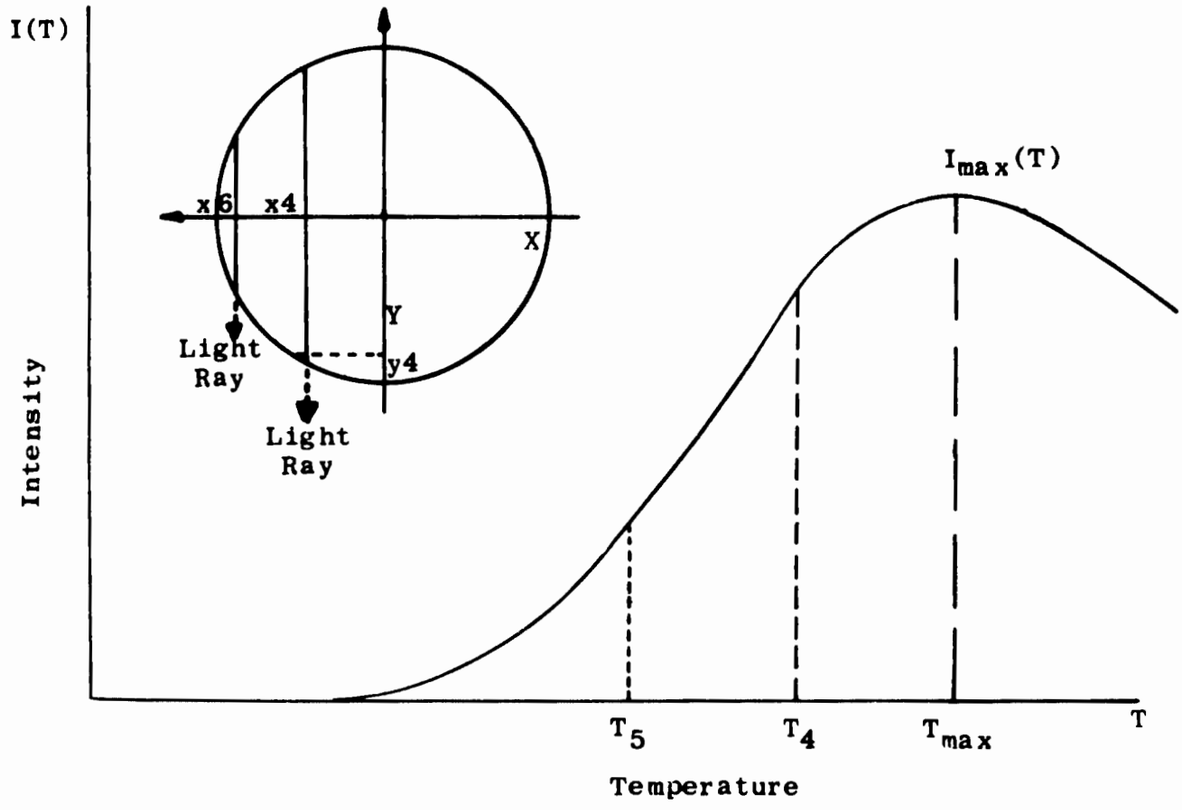

Figure20- Spectral Intensity as a Function of Temperature, Schematic

* We use the term "laminar equivalent" with the meaning "of the same average temperature".

In the I(X) distribution of a spectral line the outside parts are therefore brighter than they should be. Somewhere in the middle of the arc around T_4 one gets a correct I(X) value and finally for values still closer to the maximum of the I(T) curve too low values of line brightness I(X) will be found.

The distribution I(X) found in a turbulent arc is therefore flatter than that of the equivalent laminar arc. The deviation is stronger for a larger amplitude of the turbulent fluctuations. Also the distribution I(r), which is derived from such a turbulent distribution I(X), is then flatter than the equivalent laminar one; therefore, in turbulent arcs one measures with the method of the line intensity a somewhat too flat temperature distribution T(r) if corrections are not applied.

There is another interesting point in the curve of the temperature dependency of the spectral line intensity I(T); namely the maximum value, (I_{max}). Fluctuations, as is easily seen, lower the observed maximum value substantially, but they do not shift its location T_{max} by much. If one uses therefore the peaking method of Milne-Larentz (18, 19) for a temperature measurement, a peak temperature close to the correct temperature value is found ever in turbulent arcs (20).

If one wishes to correct for errors introduced in the above discussed way in measurements of the line intensity in turbulent plasmas, one needs to know the amplitude of the turbulent fluctuations. With this amplitude, or better the spectrum of amplitudes known, a numerical analysis of the error in flattening the average T(r) distribution might be accomplished.

In this paper we have not yet determined the amplitudes of the turbulent fluctuations and therefore we can only place a rough estimate on the error of our turbulent temperature measurement.

4.412 Spectroscopic Instrumentation

The temperature measurements were performed with the methods of photographic spectroscopy. In this procedure a spectrum is taken on a photographic plate together with a frequency and with an intensity scale. Subsequently the intensity of the spectral line is derived from the blackening of that plate as measured by a microphotometer.

The spectrographic plates were taken with a Jarrell-Ash 3.4 meter plain grating spectrograph in first order. The dispersion of this instrument is 5Å/mm, in first order, the aperture is f:32 Front surface mirror optics was used throughout our optical setup (Figure 21), which had also two quartz windows between the arc and first mirror (Figure 22). Thus, ultraviolet spectra could be taken. Our intensity standard was the anode crater of the carbon arc, which according to measurements of Null and Lozier (21), radiates with an intensity of 98% of that of a blackbody radiator with a temperature of 3800°K. For wavelength calibration a mercury-cadmium spectral lamp was used.

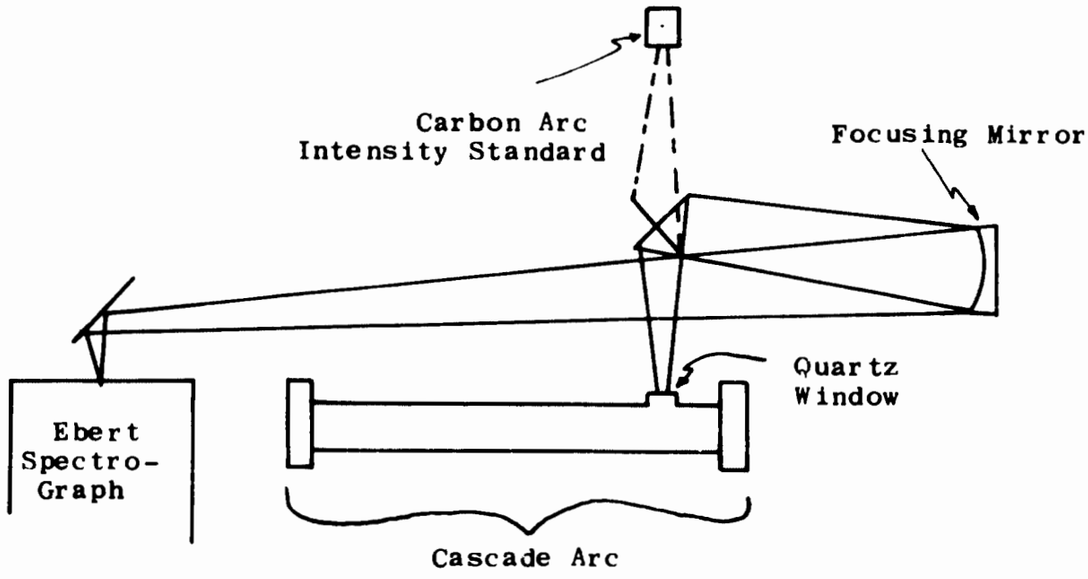

Figure 21 - Optical Ensemble for Photography of Arc and Intensity Standard, Schematic Drawing

The intensity steps of the carbon crater were made by geometric apertures which were placed into the parallel path of the spectrograph. The carbon crater was photographed with a great number of different apertures to provide for a large intensity scale. The spectrum of the test arc, however was taken without such apertures with the full grating,

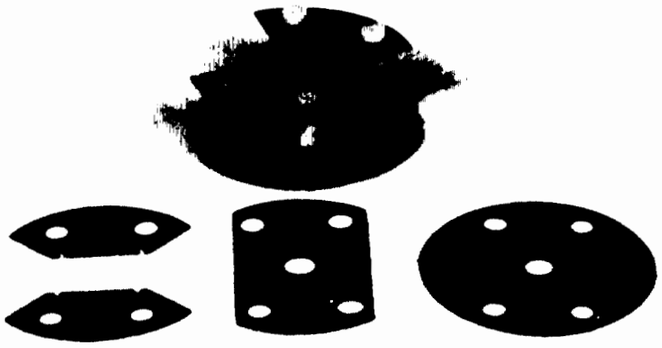

Figure 22 - Components of Spectral Window

The flat quartz window provides a view of a 2mm length of the arc. The surrounding copper discs are cut back to provide a full optical view.

Figure 22a - View of Spectral Window in Place

An outer quartz plate with "O-ring" seals the high pressure; the inner quartz keeps the arc from expanding into the dead volume between the quartz plates. Disc thickness is limited to 0.5mm by the high potential gradients of nitrogen arcs.

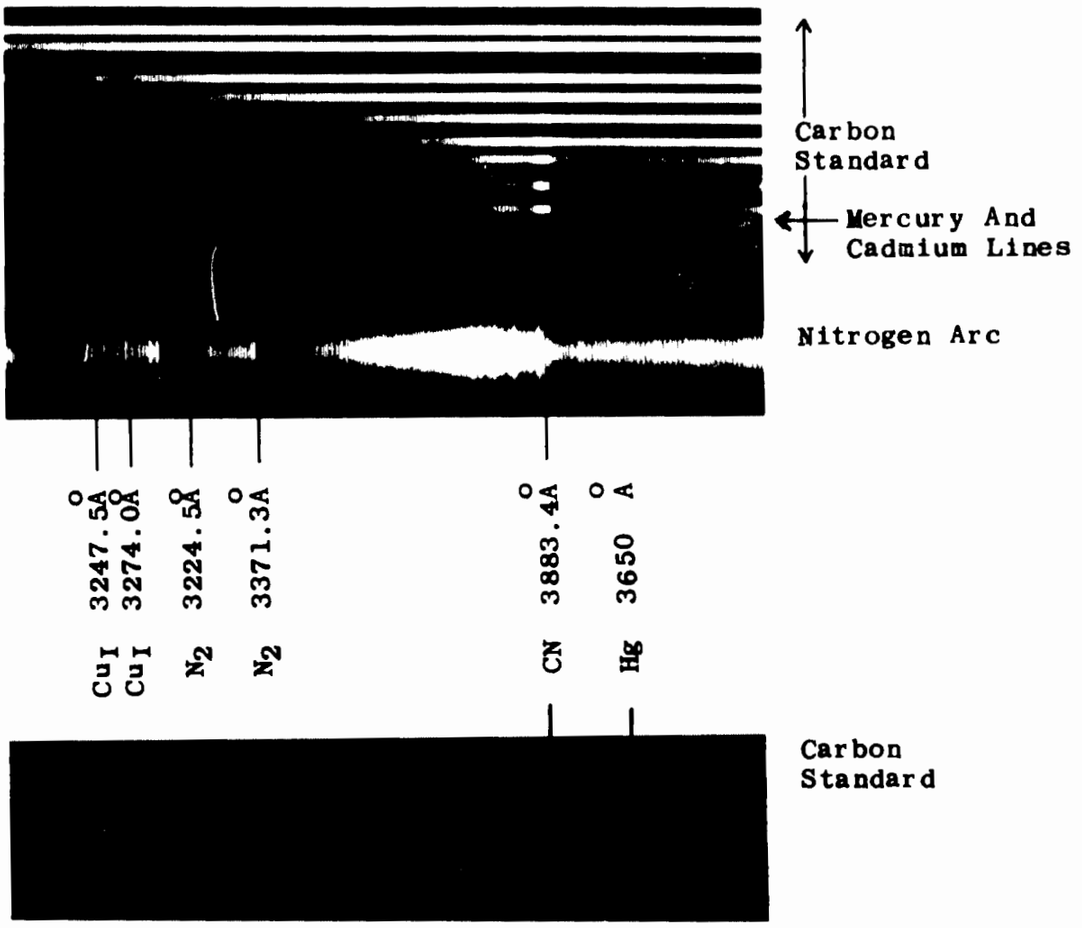

Figure 23 - Example of Photographic Plate Showing N_2 Band-Line 3224.5Å on Which Temperature Measurements were Made. Also shown Continuous Spectra of Carbon Standard, Which Serve as Measure for Intensity.

so that maximum resolution was obtained for the lines of this spectrum. An example of a photographic plate taken in the spectral area of the interesting N_2 band, λ = 3371Å,

is shown in Figure 23. Spectra as the one shown were then evaluated with the microphotometer.* This instrument essentially compares, at the same wavelength, the photographic density of the spectral line in question with the photographic density of the crater spectrum, which in turn represents the continuous radiation of a blackbody of 3800°K. The microphotometer is capable of examining an area on the spectral plate as small as 0.1mm x 0.01mm. Since the optical system magnifies the 7mm arc a factor of 1.9, there is no problem in resolving sections of the arc.—We have used the following photographic material and processes: Kodak 103F plates, developed at 20°C. in full strength Dektol for three minutes.

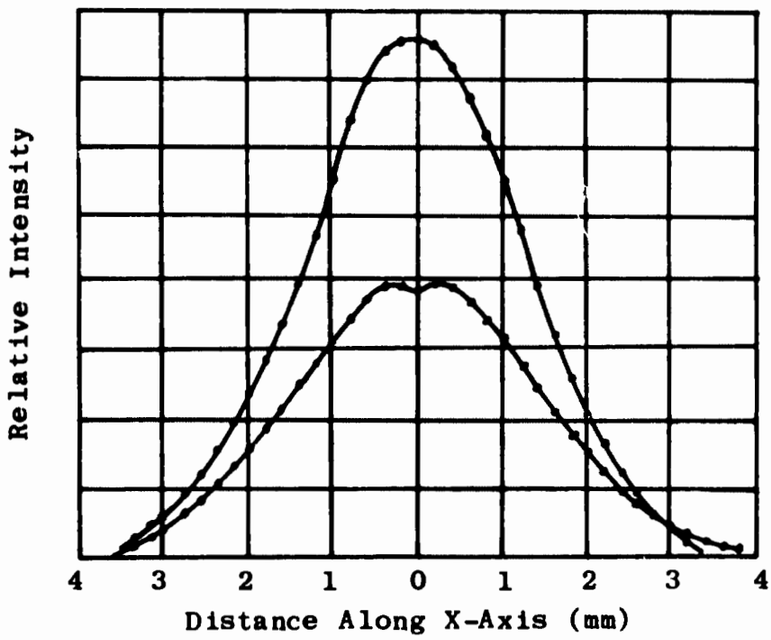

Figure 24 - Intensity Distribution Before Abel Inversion. Upper Curve is 3224.5Å Line as Read From Microdensitometer; Bottom Curve is Line After Continuous Background is Subtracted.

* National Spectrographic Laboratories

4.413 Specific Problems

A specific problem in the spectroscopic measurements was the relative weakness of the nitrogen band spectrum as compared to the strong underlying continuous radiation of the high pressure nitrogen arc. It was the strength of the continuum which persuaded us to make the first temperature measurements at an arc of relatively low current, namely of about 40 amps. Even at this current the continuum contributes about 50% of the total signal, and has therefore to be taken carefully into account.

The I(r) distribution of the line is then computed from I(X) of the line with help of the well known "Abel technique", (22). We would like to recall shortly the important relationships between I(X) and I(r), namely:

$$I(x) = 2\int_x^R \frac{I(r)\,r\,dr}{\sqrt{r^2 - x^2}}$$

and

$$I(r) = -\frac{1}{\pi}\int_r^R \frac{I'(x)\,dx}{\sqrt{x^2 - r^2}}$$

The "transformation" is, as usual, accomplished by numerical methods on a computer. From the I(r) curve and additionally from the theoretically known relationship between line intensity and temperature, (derived in the next section) the radial temperature distribution T(r) is then directly obtained.

4.414 Calculation of Relative N_2 Band Line Intensity

Considering the results of Section 4.411 about light fluctuations, the Milne-Larentz peaking method appears to give the best results for a temperature measurement in a turbulent arc in side on observation, if corrections for the fluctuations cannot be made. Therefore, in this section, the relative intensity distribution of the N_2 band $\lambda = 3371.3\text{Å}$ is calculated.

The relative temperature dependence of the intensity of a spectral line is described by the following relation:

$$I(T) \approx \frac{n_o(T)\exp\left(\frac{-\varphi}{BT}\right)}{Z_o(T)}$$

where n_o is the density of the radiating "system" (atom molecule, ion), φ is the excitation energy of the upper energy level, B = Boltzman's constant, T = absolute temperature, and Z_o is the partition function of the system. For the N_2 band with band head at λ = 3371.3Å, φ is 11.03 electron volts. The density of nitrogen molecules under 5, 10, 11.2, and 20 atmospheres pressure at 200°K intervals was determined by interpolation from the calculations of Hilsenrath and Klein, (23). The partition function was calculated on a computer using the approximation of Fast, (24), also at 200°K intervals. The results are given below:

TABLE II

T	Z_o	T	Z_o
6,000	2,530	9,200	5,590
6,200	2,680	9,400	5,830
6,400	2,840	9,600	6,080
6,600	3,000	9,800	6,320
6,800	3,170	10,000	6,580
7,000	3,340	10,200	6,840
7,200	3,520	10,400	7,100
7,400	3,710	10,600	7,390
7,600	3,890	10,800	7,670
7,800	4,090	11,000	9,560
8,000	4,290	11,200	8,260
8,200	4,490	11,400	8,570
8,400	4,700	11,600	8,880
8,600	4,910	11,800	9,200
8,800	5,130	12,000	9,530
9,000	5,360		

With these values the curve of Figure 25 was calculated for 11.2 atmospheres; maximum intensity is at 9,300°K. At higher pressures this maximum shifts to higher temperatures. This dependence on pressure is shown in Figure 26, where the temperature of maximum intensity is given.

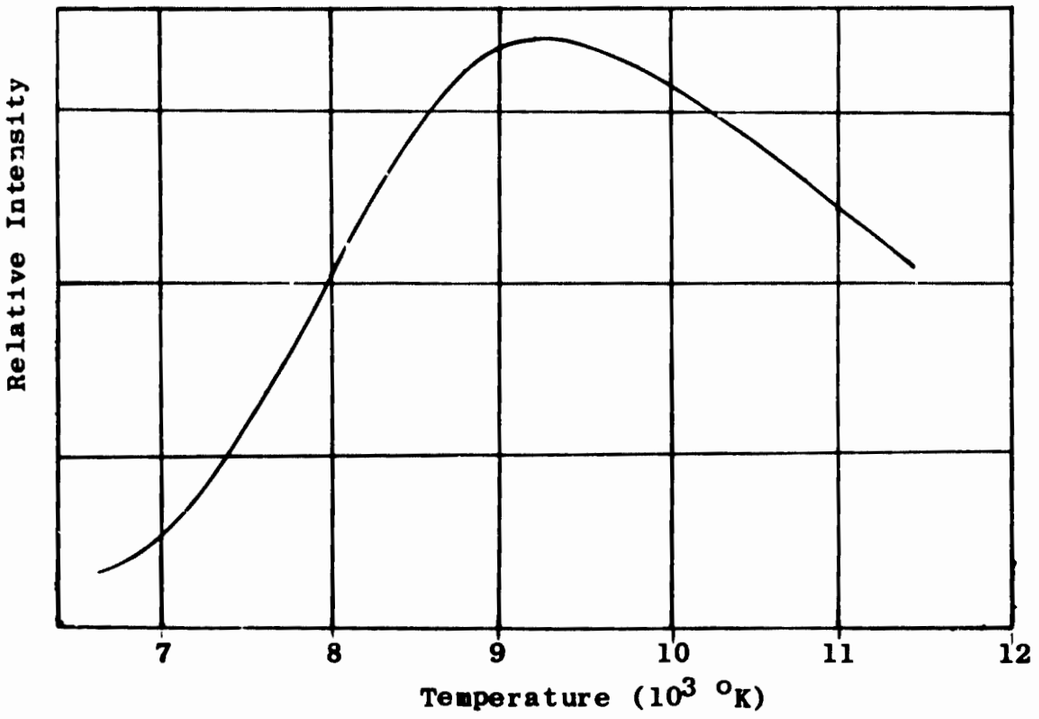

Figure 25 - Relative Intensity of λ = 3371Å N_2 Band Lines as a Function of Temperature

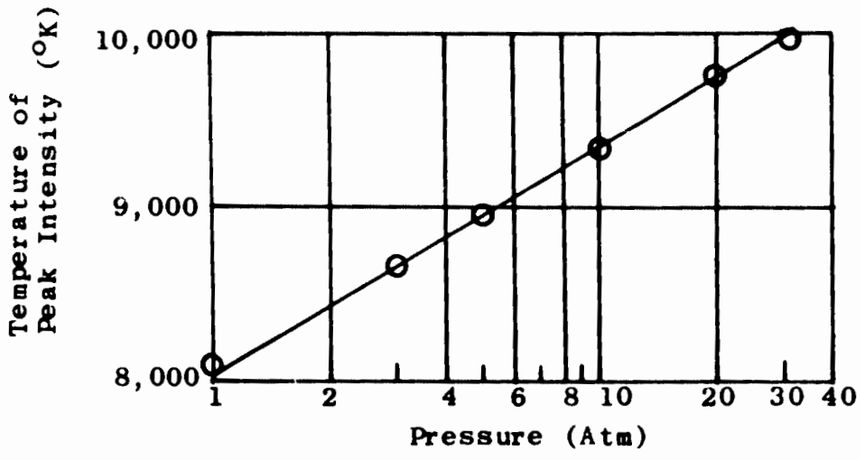

Figure 26 - Variation of 3371Å N_2 Band Line Intensity Maximum With Pressure

4.42 Results

4.421 Temperature of a 50 Amp. 11.2 Atm. Laminar N_2 Arc

It is valuable to know first the laminar temperature distribution before one measures the turbulent one.

We chose the 50 amp. N_2 arc as the vehicle for our study, because preliminary spectrograms showed that the nitrogen band lines of the 3371Å band stand sufficiently clear against the background continuum at this current and at the high pressure of 11.2 atm. Also, we were able to take, at these conditions of current and pressure, good spectrograms of the spectra of a turbulent arc.

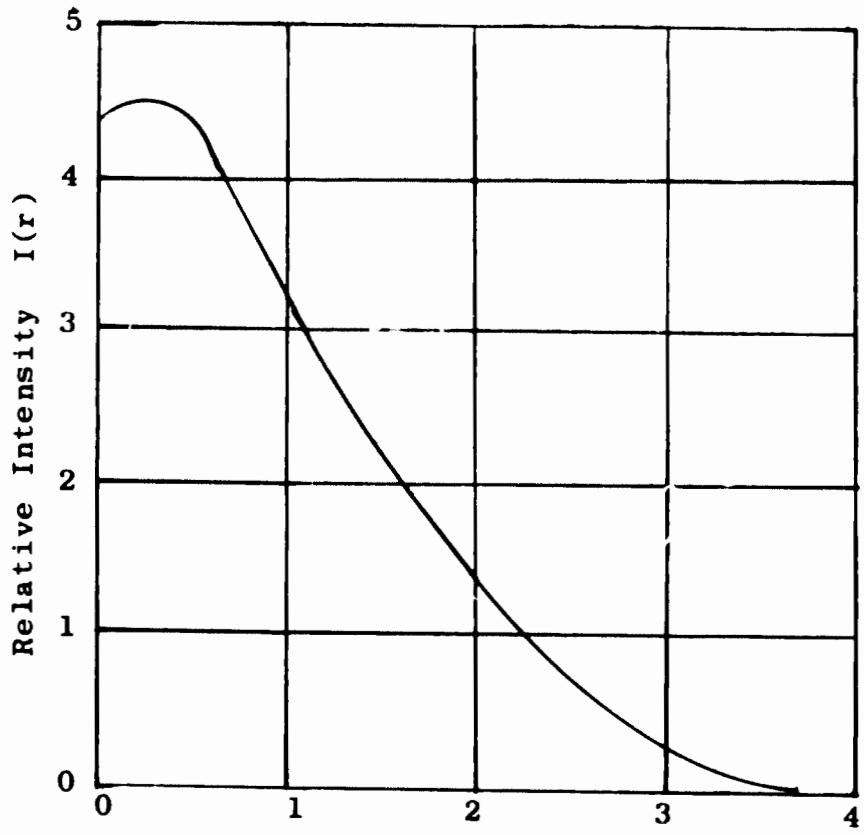

Figure 27 - Line Intensity vs Radius as Determined by Abel Inversion of I(x)

Tube Diameter:	0.7 cm
Window Diameter:	1.0 cm
Tube Length:	50 cm
Length to Window:	43 cm
Current:	50 Amps
Gas:	Nitrogen
Pressure:	11.2 Atm.
Spectral Line:	3324.5Å
Test #:	237

A typical result of a radial intensity distribution I(r), which was produced by applying the Abel technique to the primarily measured intensity distribution I(X), is shown in Figure 27. The intensity I(r) shows the Milne-Larentz maximum in this case in the very close neighborhood of the arc axis, indicating that the peak arc temperature lies only slightly higher than 9,300°K. A radial temperature distribution in the arc can then be derived by comparing the experimental curve of Figure 27 and the theoretical result of Figure 25. One starts with the "absolute" temperature point 9,300°K at radius 0.2mm and calculates then the relative temperature distribution following both curves to the outside and also to the inside. The results of this process are shown in Figure 28.

The flatness of the Milne-Larentz maximum does not lead to a precision measurement. We estimate therefore, the uncertainty of our measured axial temperature to be ± 500°K.

4.422 Temperature of a Turbulent 50 Amp., 11.2 Atm. Nitrogen Arc

The temperature of a turbulent 50 amp. arc in 11.2 Atm. of nitrogen was measured in the same way as that of the laminar arc in the last section. The relative intensity distribution I(r) of the nitrogen band lines was very similar to that of the laminar arc and it led therefore to nearly the same axis temperature. Actually, as discussed in Section 4.411, the Milne maximum will not be at exactly the same "average" temperature in the turbulent case, as in the laminar arc. We can at this time, however, not make a correction of this, because we have no information about the amplitude of the turbulent light fluctuations. Knowledge of this amplitude is therefore desirable in the future. Further in all points except the Milne maximum, the average brilliancy of the lines will only be approximately representative for the average temperature as discussed earlier in detail. In spite of this we have calculated the radial temperature distribution in the turbulent arc from its I(r) distribution and arrived at the values of Table III, in which T_{lam} and T_{turb} are the temperatures in the respective 50 amp. arcs.

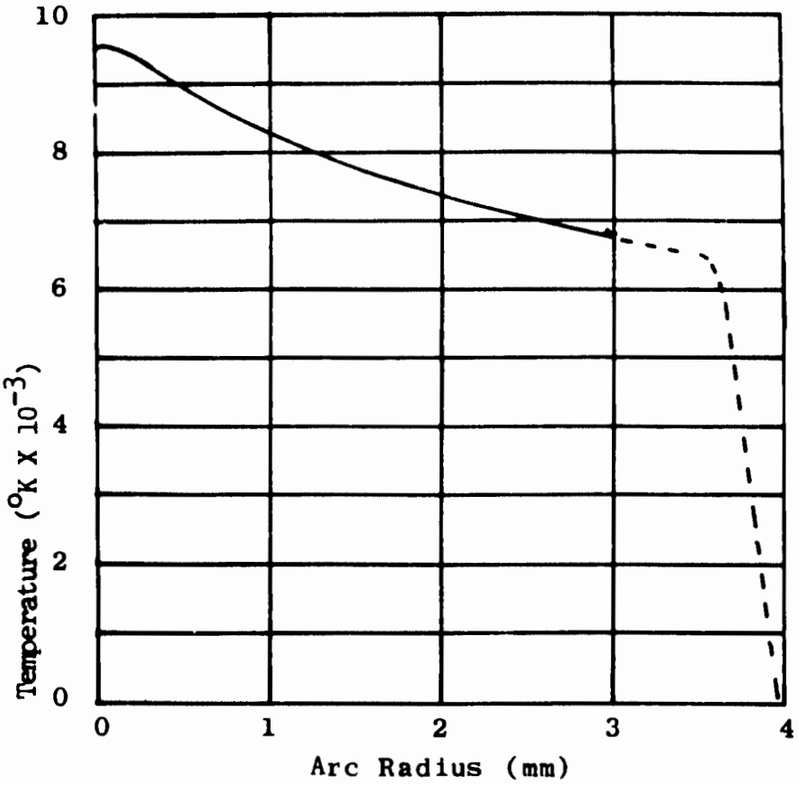

Figure 28 - Radial Temperature Distribution of a 50 Ampere Nitrogen Arc (Laminar Regime)

Tube Diameter:	0.7 cm; 1 cm at Window
Tube Length:	50 cm
Length to Window:	43 cm
Current:	50 Amp.
Pressure:	11.2 Atm.
Gas:	Nitrogen
Flow Rate:	0.1 gr/sec.
Test #:	239

TABLE III

r	0	0.2	0.4	0.6	0.8	1.0	1.2	1.4	1.6	1.8	2.0	(mm)
T_{Lam}	9500	9400	9000	8700	8490	8300	8125	7950	7760	7600	7420	°K
T_{Turb}	9700	9620	9300	8900	8550	8450	8240	7950	7750	7500	7350	°K

r	2.2	2.4	2.6	2.8	3.0	3.2	(mm)
T_{Lam}	7240	7100	6950	6760	6700	6580	°K
T_{Turb}	7200	7100	6950				°K

Obviously, for the outer parts of the arc, one more independent absolute temperature point would help to give confidence to the measured values of the turbulent temperature distribution. We will therefore, in future measurements, use for such a measurement the Milne maximum of sodium lines as done by Maecker, (25).

To support the measured value, 9,700°K, in the arc axis of the turbulent arc, we refer to the result of a second measurement. We determined the absolute intensity of the continuous radiation at the wavelength 5218Å in all our laminar and also in our turbulent measurements. Two results were obtained. First, the absolute intensity at the arc axis reproduced in the laminar shots within ± 10%. Second, the absolute intensity of the continuous radiation in the turbulent measurements was 60% ± 10% of the laminar value. This difference might be considered large. Assuming, however, for the matter of argument, that the majority of the continuous radiation is recombination and is "Bremsstrahlung"; we calculate that a temperature difference of only 350° is enough to explain the measured intensity difference.*

* The reason for this small temperature difference is the sharp increase of recombination radiation with temperature. The electron densities for this calculation were taken from (23).

It appears therefore that the average temperature in the axis of the turbulent 50 amp. N_2 arc can indeed be only slightly different from that in the laminar 50 amp. arc in nitrogen.

4.423 Determination of Copper Contamination

In addition to the previously reported temperature measurements, a spectroscopic determination of the contamination of the 50 amp. N_2 arcs with copper atoms was made. This was done by measuring the absolute intensity of the copper line 5218Å, of which the transition probability is known (26). The copper contamination fluctuated from shot to shot; but was, however, very low in all measurements. We obtained a partial copper pressure of 100-500 dynes/cm^2 for the laminar 50 amp. N_2 arc and 1500 dynes/cm^2 for the turbulent N_2 arc. This is a Cu contamination of less than 2 in 10^4 parts of nitrogen.

5. CONCLUSIONS

Our work on turbulent arcs has increasingly progressed toward a quantitative stage. To achieve this, work on several diagnostical methods was pursued and the following results were obtained:

5.1 The plasma pressure could be measured along a flow tube in our transient measurements. The important cold flow relationship that the pressure gradient is in turbulent flow proportional to the 1.8 power of the flow rate was found to be true also in a fast flowing high temperature argon arc of 125 amp. and 11.2 atm.

5.2 The plasma velocity near the arc axis was measured and found to be proportional to the flow rate in an argon arc. Therefore, the pressure gradient in the high speed argon arc was also proportional to the 1.8 power of the plasma velocity.

5.3 Work on a method to measure <u>average</u> <u>turbulent</u> temperatures led to the following results:

5.31 It was theoretically demonstrated that correct average temperature measurements can be made in "end on" observation, if spectral lines are used in the "inflection" point of their I(T) curve.*

* For details see Section 4.411

5.32 A method was outlined which allows one to measure average turbulent temperatures also "side on". This method, however, has still to be quantitatively developed.

5.33 Temperature measurements were made on 11.2 atm. nitrogen arcs of about 50 amps in laminar and in turbulent flow. Although the turbulent measurement must still be considered as preliminary, it indicates strongly that both arcs have closely the same average axis temperature and also a similar radial temperature distribution.

5.34 Measurements of the arc characteristics in 11.2 atm of argon and nitrogen in a 7mm tube showed a wide separation of the laminar and the turbulent characteristics even at currents as high as 200 amps.

5.36 Calculations indicated that total radial heat flux can be measured with a calorimetric method.

Whereas the described methods and measurements have not yet led to a comprehensive description of one particular turbulent situation, they have increased our understanding of the conditions in turbulent arcs significantly and show promise for further development.

6. FUTURE WORK

Future work will be directed toward a group of measurements, which allow the correlating of turbulent energy and momentum transfer in the fully developed flow section of electric arcs with non-dimensional quantities of the flow and temperature field. To achieve this, our diagnostic methods for the measurement of temperature, flow velocity and radiative heat flux have to be further improved.

APPENDIX*

Design calculations were made on a radiant flux calorimeter similar to one used for a study of high pressure arc radiation, (27) shown schematically in Figure 29. A small copper ring exposed to arc radiation but shielded as much as possible from thermal conduction serves as a calorimeter. Total temperature rise for time of arc duration is measured after arc extinction to avoid the necessity of primary arc voltage.

The calorimeter assembly is in the form of a sandwich with one of the copper constrictor discs replaced by the thermally insulated calorimeter ring. The longer operating time** presents a special problem in that a substantial temperature rise in the adjacent copper discs has time to diffuse some distance radially, (Figure 30).

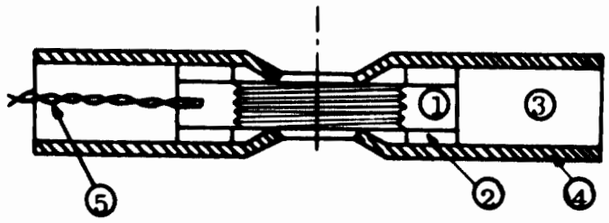

Not to Scale

① Copper Ring Sensing Element
② Alumina Ceramic
③ Plexiglas Spacer Disc
④ Copper Disc
⑤ Thermocouple

Figure 29 - Section Drawing of Total Radiation Calorimeter

* The symbols of this section are explained in the text.

** Typically 50-100 msec. versus 2 msec. for the high pressure arc.

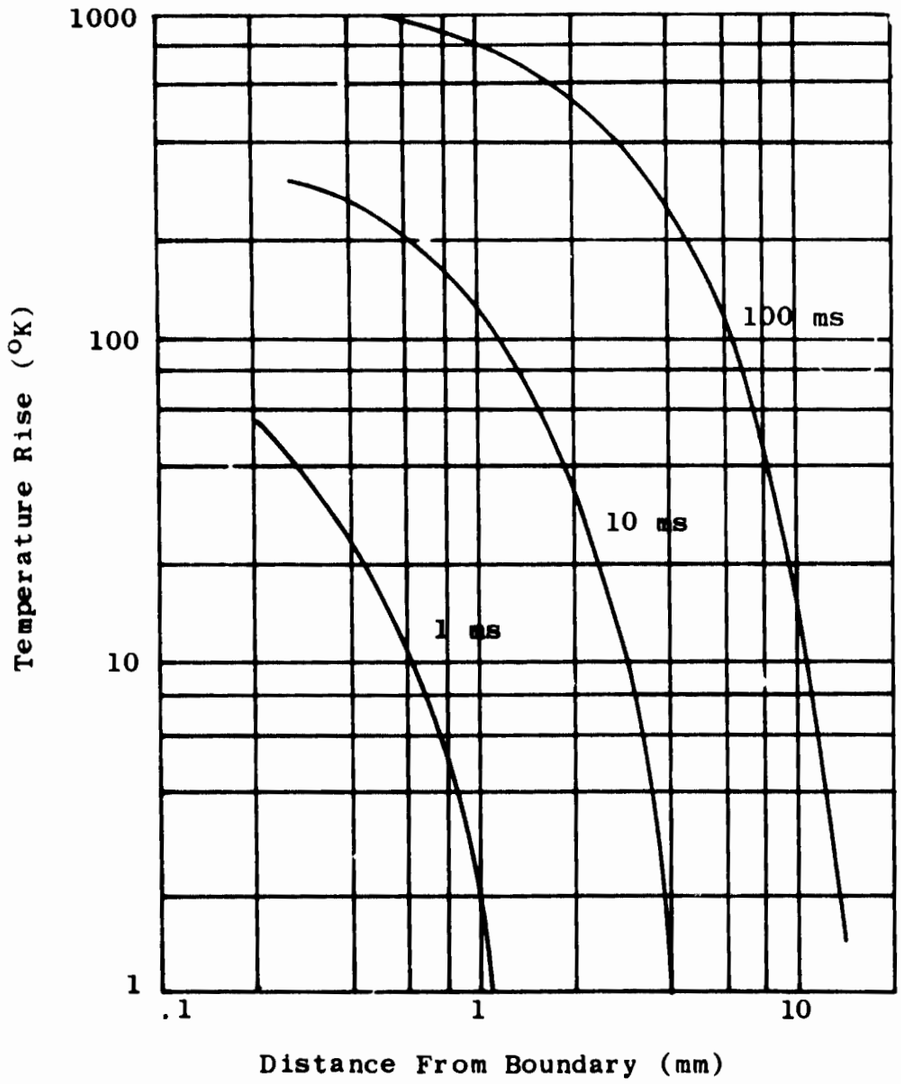

Figure 30 - Temperature Rise in a Semi-infinite Solid With Constant Heat Flux at the Boundary

Material: Copper
Heat Flux: 10kw/cm^2

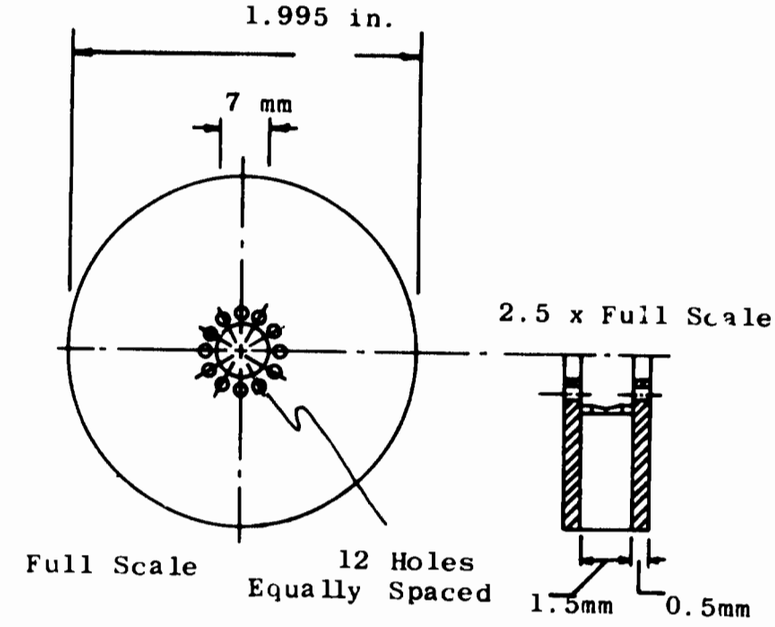

Figure 31- Tentative Calorimeter Design With Blocking Holes

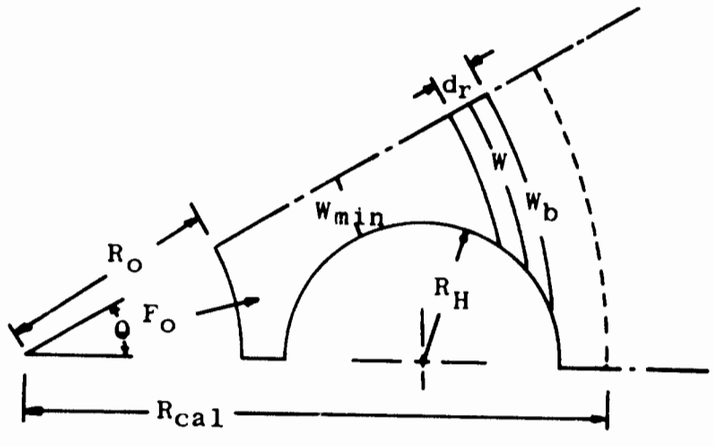

Figure 32 - Heat Conducting Path For Calorimeter With Blocking Holes. The Critical Parameter is the Ratio of W_{min} to $(W_{min} + R_H)$.

To block thermal conduction, the possibility of reducing the conducting area by drilling a ring of holes in the copper disc as shown in the tentative design sketch, Figure 31, was investigated. For this purpose a computer program was written to study transient thermal behavior when a constant heat flux is applied to the inner edge. The heat flux within the copper was considered to be one-dimensional in the same sense that fluid flow in a channel of varying cross section is considered one-dimensional, that is, heat flux through any section of path width W, was assumed uniform and a function of time only. The blocking holes are uniformly spaced, so, by symmetry the conduction path of interest is that shown in Figure 32. The path width is a function of r only.

First temperature distribution is computed for a semi-infinite solid at a time t_o such that thermal penetration thickness $\delta_T = 4\sqrt{\alpha t}$ where $\alpha = K/\rho c$ * is less than the thickness of the copper disc 4 from Figure 29. The following difference equations were used for computing the time dependent temperature distributions.

$$T_1' = T_1 + G/W_1\left[\frac{F_o R_o \theta \Delta r}{K} - W_{b1}(T_1 - T_2)\right]$$

$(n=1)$

$$T_n' = T_n + G/W_n\left[W_{b_{n-1}}(T_{n-1} - T_n) - W_{bn}(T_n - T_{n+1})\right]$$

$(n>1)$

Here F_o is the heat flux at R_o, $G = \alpha \Delta t/(\Delta r)^2$ (for stability $G \leq 0.5$) W_b is the path width at the boundary of an element and the prime signifies temperature at time $t + \Delta t$.

Result: Figures 33 and 34 show that to be effective, the path width ratio must be very small, which reduces the time to surface melting. Figure 33 is based on an assumed thermal load of 10Kw/cm^2. This is a high value compared to these which we report upon in Section 4.1. For lower thermal loads the "operational" times should be considerably longer. The time to surface melting will be approximately inversely proportional to the square of the heat load.

* C is Here Specific Heat.

** $\theta = \frac{\pi}{12}$ See Figure 32

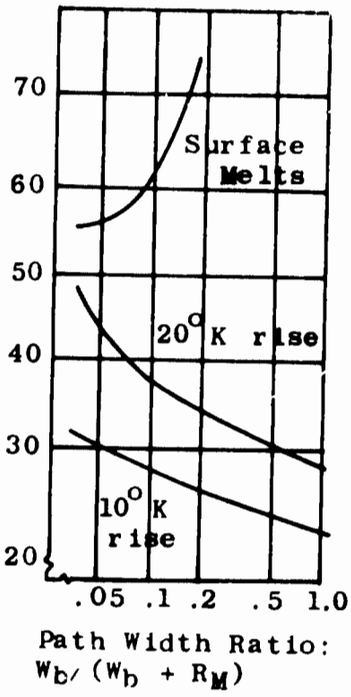

Figure 33 - Temperature Rise as a Function of Path Width Ratio

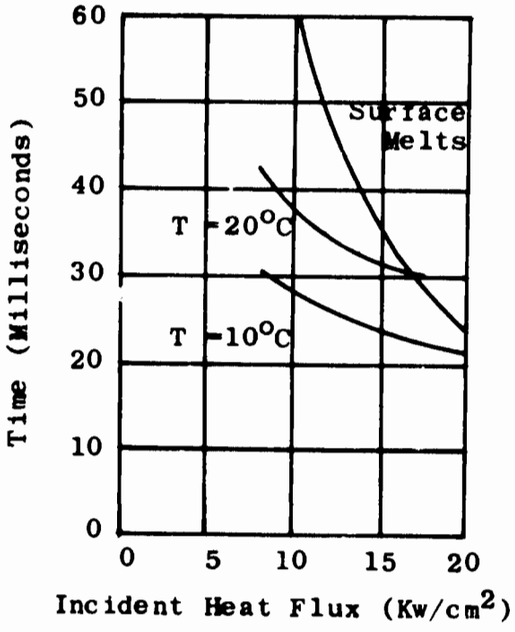

Figure 34 - Temperature Rise as a Function of Incident Heat Flux

REFERENCES

1. Cobine, J. D: Gaseous Conductors, Dover Publications, New York, 1957.

2. Encyclopedia of Physics, Flügge, ed, Finkelnburg. W. and Maecker, H., Electric Arcs and Thermal Plasma, Vol. XXII, Gas Discharges II, Pages 254ff. (In German). Springer-Verlag-Berlin.

3. Skilstad, J.G: Summary of Published Literature Concerned with Electric Arc Phenomena Pertinent to Plasma Jet Devices Report No: TM-62-4, Jet Propulsion Center, Purdue University, 1962.

4. John, R. R. and Bade, W. L: Recent Advances in Electric Arc Generation Technology, ARS - Journal, 31, 4-17, 1961

5. Runstadler, P.W: Laminar and Turbulent Flow of an Argon Arc Plasma, Technical Report No. 22, Div. of Eng. and Applied Physics, Harvard University, 1965.

6. Frind, G: Electric Arcs in Turbulent Flows, II, Aerospace Research Laboratory Report, ARL 66-0073, 1966.

7. Granatstein, V. L. and Buchsbaum, S. J: Turbulent Mixing in a Laboratory Plasma, Appl. Phys. Letter 7, 285-287, 1965.

8. Yos, J: In article: Theoretical and Experimental Investigation of Arc Plasma Generation Technology, Part II, Vol. 2, ASD, TDR-62-729, Part II, Vol. 2, 1963.

9. Burhorn, F. and Wienecke, R: Plasma Composition, Plasma Density, Enthalpy, and Specific Heat of Nitrogen, Nitrogen Monoxsyd and Air at 1; 3; 10 and 30 atm. in the Temperature Range between 1,000 and 30,000°K (In German) Zeit. Phys. Chem. 215, 269-284 1960.

10. Cann, G. L: Energy Transfer Processes in a Partly Ionized Gas, Guggenheim Aero. Lab. Cal. Tech. Memo No. 61, 1961.

11. Penski, K: Chemie - Ingenieur Technik 34, 84-87, 1962, (In German).

12. Rohsenow, W. M. and Choi, H. Y: Heat, Mass and Momentum Transfer, Prentice Hall, Inc., Englewood Cliffs, N. J., 1961 pages 47ff; 168ff.

13. Elenbaas, W: The High Pressure Mercury Vapor Discharge, North Holland Publ. Co., Amsterdam, 1951

14. Maecker, H: About the Characteristics of Cylindrical Arcs, Zeit. Phys. 157, 1-29, 1959. (In German)

15. Bauer, A: An Approximate Solution of the Elenbaas-Heller Differential Equation, Zeit. Ang. Phys., 15, 550-556, 1963 (In German).

16. Barkan, P. and Whitman, A. M: An Uncooled, Rapid Response Probe for Measuring Stagnation Pressures in High Velocity Plasma, Aerospace Research Lab. Report No. ARL 64-192, 1964.

17. Reference 12, Pages 56-59.

18. Fowler, R. H. and Milne, E.A: The Intensity of Absorption Lines in Stellar Spectra, and the Temperatures and Pressures of the Reversing Layers of Stars.
Mon. Not. Roy. Astr. Soc. 83, 403-424, 1923
Mon. Not. Roy. Astr. Soc. 84, 499-515, 1924

19. Larentz, R.W: A Method for the Measurement in Optically Thin Arc Columns. Zeit. Phys. 129, 327-342, 1951, Zeit. Phys. 129, 343-364, 1951. (In German).

20. Burhorn, F. and Altera: Temperature Measurements on Water Stabilized High Current Arcs. Zeit, Phys. 131, 28-40, 1951, (In German).

21. Null, M. R. and Lozier, W. W: Carbon Arc as a Radiation Standard, J. Opt. Soc. Am. 52, 1156-1162, 1962.

22. Cremers, C. J: The Spectrometric Measurement of the Temperature Field in an Arc with a Transpiration-Cooled Anode; Aerospace Research Laboratories Report ARL 65-117, 1965.

23. Hilsenrath, J. and Klein, M: (Table of Thermodynamic Properties and Chemical Compositition of Nitrogen), Arnold Eng. Dev. Center, Rep. TR-66-65, 1966.

24. Fast, J. D: The Dissociation of Nitrogen in the Welding Arc, Philips Res. Rep. 2, 382, 1947.

REFERENCES (Cont'd)

25. Maecker, H: Electron Density and Temperature in the Column of the High Current Carbon Arc, Zeit. Phys., 136, 119-136, 1953.

26. Allen, C. W: Astrophysical Quantities, Second Ed., University of London Press, 1964.

27. Marston, C. H: et Altera., Radiation Heat Flux From High Pressure Air Arcs, Report AEDC-TR-66 258, 1966.

Unclassified
Security Classification

DOCUMENT CONTROL DATA - R & D

(Security classification of title, body of abstract and indexing annotation must be entered when the overall report is classified)

1. ORIGINATING ACTIVITY (Corporate author) General Electric Company 6901 Elmwood Avenue Philadelphia, Pennsylvania 19142	2a. REPORT SECURITY CLASSIFICATION Unclassified 2b. GROUP

3. REPORT TITLE

Electric Arcs in Turbulent Flows, III

4. DESCRIPTIVE NOTES (Type of report and inclusive dates)
Scientific. Interim.

5. AUTHOR(S) (First name, middle initial, last name)
Gerhard Frind
Ben Lee Damsky

6. REPORT DATE April 1968	7a. TOTAL NO OF PAGES 50	7b. NO. OF REFS 27
8a. CONTRACT OR GRANT NO. F33615 67 C 1374 b. PROJECT NO. 7063 c. DoD Element 6144501F d. DoD Subelement 681307	9a. ORIGINATOR'S REPORT NUMBER(S) 9b. OTHER REPORT NO(S) (Any other numbers that may be assigned this report) ARL 68-0067	

10. DISTRIBUTION STATEMENT
This document has been approved for public release and sale; its distribution is unlimited.

11. SUPPLEMENTARY NOTES TECH OTHER	12. SPONSORING MILITARY ACTIVITY Aerospace Research Laboratories (ARN) WPAFB, Ohio 45433

13. ABSTRACT

Work is reported on the development of methods to measure arc temperature, axial pressure gradient, plasma flow velocity and radiative heat flux in long cylindrical turbulent arcs.

Axis temperature and radial temperature distribution of laminar and turbulent 50 amp. nitrogen arcs of 11.2 atm. pressure were found to be of similar size, with some reservation about the accuracy of the "side on" turbulent temperature measurement. The problem of measuring average turbulent arc temperatures was discussed; measurements in "end on" observation and the use of the Milne-Larentz method appear to give better results than "side on" observation of absolute line intensities.

Measurements of the pressure gradient in a 11.2 atm., 125 amp. argon arc show a 1.8 power dependence of pressure gradient on flow rate, indicating that this relationship, well known from cold flow experiments, also holds under the conditions of our experimental arc temperatures.

Plasma velocities were measured by time sequential photography of the turbulent arc structure.

DD FORM 1 NOV 65 1473

Unclassified
Security Classification